Scattering by Nonspherical Systems*

by

J. Mayo Greenberg†, Arthur C. Lind, Ru T. Wang
Rensselaer Polytechnic Institute, Troy, New York

and

Louis F. Libelo‡
U. S. Naval Ordnance Laboratory, White Oak, Maryland

GPO PRICE $ _____

CFSTI PRICE(S) $ _____

Hard copy (HC) 3.00

Microfiche (MF) .50

ff 653 July 65

*Work Supported by grants from the National Aeronautics and Space Administration and the National Science Foundation.

†Currently on leave of absence as a member at the Institute for Advanced Study, Princeton, New Jersey.

‡Part of this paper is taken from a thesis submitted by L. F. Libelo in partial fulfillment of the degree of Doctor of Philosophy at Rensselaer Polytechnic Institute.

FACILITY FORM 602

N66-13012 (ACCESSION NUMBER) (THRU)

54 (PAGES) 1 (CODE)

CR-68293 (NASA CR OR TMX OR AD NUMBER) 24 (CATEGORY)

Abstract

13012

Theoretical and experimental results on the scattering by nonspherical particles whose size is of the order of the wave length are presented.

A method of solution of the problem of scattering by axially symmetric penetrable particles using approximate matching of boundary conditions is applied to the scattering by prolate spheroids. Application is made specifically to the scattering of a scalar wave incident along the symmetry axis. In comparison with exact scattering coefficients for the sphere, it is shown that the "approximate" method yields results as close as one wishes to the exact results. Calculations are presented for particle sizes ranging from those small enough to be calculated by the Rayleigh approximation to sizes generally beyond the first major resonance in the total cross-section curve.

Numerical calculations are made for the tilted infinite dielectric cylinder. Some new and interesting properties of the scattering efficiency as a function of orientation are demonstrated. Particularly noted is the existence of a polarization reversal as a consequence of tilt for thin cylinders.

A new and improved method for obtaining microwave scattering by small particles is applied to the consideration of the detailed dependence on orientation of the cross-section of prolate spheroidal particles. The particle sizes range from slightly beyond the Rayleigh approximation to somewhat larger than the first major resonance in the extinction curve. The results are, where appropriate, compared with the Rayleigh approximation and a simple ray approximation. The ray approximation is shown to yield better results in certain cases than had been anticipated although there exists an intermediate but reasonably defined span of particle sizes for which the approximation is even qualitatively poor.

1. Introduction

The method of scattering is applied as an investigatory tool in studies ranging from the character of atomic nuclei through sizes and shapes of large molecules to the character of disturbances in the solar corona. The demands made upon the theory of the scattering process have often not been met even for application to situations which involve well-known physical processes and basic mathematical equations. Disregarding the possibilities of complicated interactions between waves and obstacles there still are important gaps in the theoretical procedures. As a matter of fact the special case of the scattering of light by simple nonspherical particles is adequately treated only when the particles are either very small or very large compared with the wave length of light.

Van de Hulst[1] has surveyed the domain of m (m = index of refraction) and ka ($ka = 2\pi a/\lambda$, a = a characteristic linear dimension, λ = wave length) for the regions of simple approximations and simple physical interpretations. The ranges of ka and m with which we are concerned here are just those which do not satisfy the simplicity criteria. We consider here those particles for which $ka \gtrsim 1$, $(m - 1)$ <u>not</u> $\ll 1$, $2ka\,(m - 1) \gtrsim 1$; i.e., neither the Rayleigh[2] nor the Rayleigh-Gans-Born[3] approximations are applicable.

The primary aim of this paper is to report on some progress that has been made at Rensselaer in extending our range of information, both actual and potential, concerning the scattering by nonspherical sharply

bounded obstacles. We believe that the results which are present are new and that they indicate the possibilities for obtaining complete solutions to a useful range of problems in the near future. In other words, we believe that the problem of single scattering will soon be essentially solved.

The work described in the following three sections is abstracted from separate and more detailed accounts which are reported on elsewhere.

In section 2 we describe a method[4] for obtaining the numerical solution to the scattering by an axially symmetric penetrable particle whose size ranges from the very small to a value essentially limited by computing machine time. Although the problem treated here is limited to that of a scalar wave propagated along the axis of the particle, there does not appear to be any difficulty to generalize at least to the electromagnetic case. This has been done, but a formal solution and procedure are too lengthy to give here.

The numerical solution to the scattering of electromagnetic waves by an arbitrarily oriented dielectric cylinder is discussed in section 3.

In section 4 we give some results obtained by an experimental method using microwaves for the study of scattering by aribtrarily oriented penetrable spheroids. The value of the microwave method lies in its applicability to the widest range of anisotropy of shape and optical properties.

2. Solution to the Scattering Problem by Approximating Boundary Conditions

We consider here the problem of the scattering of a plane scalar wave which is incident along the axis of a smooth convex cylindrically symmetric body. The boundary conditions which we apply will correspond to the scattering of Schrödinger waves by a square well potential and to the scattering of acoustic waves by a body whose density is equal to that of the surrounding medium. Our results will thus be the scalar wave analog of the electromagnetic scattering problem.

The method of approximation is applied first to the case of the sphere as a means of checking the accuracy of the method by comparison with exact solutions. Application is then made to prolate spheroids up to elongations of two.

As we shall see, the solutions which are obtained are complete in the sense of being valid not only in the asymptotic region, but at all interior and exterior points. Furthermore it is reasonable to expect the solutions to have reliability equal to that of Mie[5] series expansions so long as appropriate restrictions are imposed on the range of applicability.

a. Outline of the computational procedure

We desire solutions to the scalar wave equation

$$\nabla^2\psi + k^2(\underline{r})\psi = 0 \qquad (1)$$

where $k(\underline{r}) = 2\pi/\lambda(\underline{r})$ is the wave number at the point $\underline{r}$. The problems which we treat will be limited to homogeneous scatterers which are

characterized by having a wave number inside, κ, which is a constant, m (index of refraction) times the wave number outside, k.

The boundary conditions on the solution are that the wave function and its normal derivative be continuous

$$\left.\begin{aligned} \psi_{\text{inside}} &= \psi_{\text{outside}} \\ \underset{\sim}{n} \cdot \nabla\psi_{\text{in}} &= \underset{\sim}{n} \cdot \nabla\psi_{\text{out}} \end{aligned}\right\} \quad \text{at the surface of the scatterer} \qquad \begin{aligned} &(2a) \\ &(2b) \end{aligned}$$

where $\underset{\sim}{n}$ is the normal to the surface.

We further impose the radiation condition

$$\psi \underset{r\to\infty}{\to} e^{ikz} + \frac{f(\theta)}{kr} e^{ikr} \qquad (2c)$$

We may expand the solutions inside and outside in the standard forms which satisfy the differential equation and the radiation condition (2c)

$$\begin{aligned} \psi_{\text{inc}} &= e^{ikz} = \sum_{\ell=0}^{\infty} (2\ell+1)\, i^{\ell}\, j_{\ell}(kr) P_{\ell}(\cos\theta) \\ \psi_{\text{sc}} &= \sum_{\ell=0}^{\infty} (2\ell+1)\, i^{\ell} A_{\ell}\, h_{\ell}^{(1)}(kr)\, P_{\ell}(\cos\theta) \qquad (3) \\ \psi_{t} &= \sum_{\ell=0}^{\infty} (2\ell+1)\, i^{\ell}\, B_{\ell}\, j_{\ell}(\kappa r)\, P_{\ell}(\cos\theta) \end{aligned}$$

where ψ_{inc} is the incident wave, ψ_{sc} is the scattered wave, ψ_t is the transmitted wave, and where $j_{\ell}(z)$ is the spherical Bessel function and $h_{\ell}^{(1)}(z)$ is the spherical Hankel function of the first kind.

It is now only necessary to impose the conditions (2a) and (2b) and to solve for the coefficients A_{ℓ} and B_{ℓ}. Note that $\psi_{\text{in}} = \psi_t$ and $\psi_{\text{out}} = \psi_{\text{inc}} + \psi_{\text{sc}}$.

In the case of the sphere these B.C. (boundary condition) equations separate and one gets an infinite set of independent pairs of equations

in the A^{l} s and B^{l} s which may be readily solved. If the bounding surface is nonspherical, the infinity of equations are coupled and a simple solution no longer exists.

The series expressions(3) are generally not rapidly converging. However, it is well known that the number of terms which are required for a good representation of the solution is of the order of $n = ka = 2\pi a/\lambda$ where a is a typical linear dimension of the scatterer. In the limit of very small scatterers it would only be necessary to find A_0 and B_0 in which case we see that the functions in equation (3) are independent of angle. For small scatterers it is then obvious that if the boundary conditions are satisfied at only one point they are automatically satisfied at all points on the surface. It is to be expected that the shorter the wave length, the more points on the boundary need to be considered. In other words, the number of points at which the boundary condition is satisfied should be at least of the same order (ka) as the number of important terms in the series expressions (3). Because of cylindrical symmetry each point corresponds of course to a circle about the symmetry axis.

Our procedure consists in choosing some finite number N of points at which to satisfy the boundary conditions (2a) or (2b) and then truncating the series so that we obtain an equal number of unknowns. We then solve the 2N inhomogeneous equations in the 2N unknowns A_ℓ and B_ℓ, $\ell = 0$ to N - 1. Each point (circle) on the boundary is represented by some angle θ. It should be noted that because of the reflective symmetry of the scatterers we have chosen, if the boundary

conditions are satisfied for a given value of θ, they are then automatically satisfied for the angle $\pi - \theta$.

We shall choose s angles θ_i in the first quadrant to define an approximation of order N = 2s. We denote the approximate solutions by

$$\begin{aligned}
\psi_{inc}^{(2s)} &= \sum_{\ell=0}^{2s-1} (2\ell + 1)\, i^{\ell}\, j_{\ell}(kr)\, P_{\ell}(\mu) \\
\psi_{sc}^{(2s)} &= \sum_{\ell=0}^{2s-1} (2\ell + 1)\, i^{\ell}\, A_{\ell}^{(2s)}\, h_{\ell}^{(1)}(kr)\, P_{\ell}(\mu) \qquad (4) \\
\psi_{t}^{(2s)} &= \sum_{\ell=0}^{2s-1} (2\ell + 1)\, i^{\ell}\, B_{\ell}^{(2s)}\, j_{\ell}(\kappa r)\, P_{\ell}(\mu)
\end{aligned}$$

where $\mu = \cos\theta$.

The boundary conditions (2a) and (2b) are to be replaced by the sets of equations

$$\psi_t^{(2s)}(\mu_i) = \psi_{inc}^{(2s)}(\mu_i) + \psi_{sc}^{(2s)}(\mu_i) \qquad (5a)$$

$$n(\mu_i) \cdot \nabla \left\{ \psi_t^{(2s)}(\mu_i) = \psi_{inc}^{(2s)}(\mu_i) + \psi_{sc}^{(2s)}(\mu_i) \right\} \qquad (5b)$$

where $\mu_i = \cos\theta_i$.

We evaluate the scattering efficiency from the optical theorem

$$Q = \frac{4\pi}{(ka)^2} \operatorname{Im}\{f(0)\}$$

which for the exact solution is given by

$$Q = -\frac{4}{(ka)^2} \sum_{\ell=0}^{\infty} (2\ell + 1)\ \operatorname{Re} A_{\ell}$$

and for the approximate solution is given by

$$Q = -\frac{4}{(ka)^2} \sum_{\ell=0}^{2s-1} (2\ell + 1) \operatorname{Re} A_{\ell}^{(2s)} \qquad (6)$$

b. Approximate scattering by a sphere

The sphere is used as a test case for the method because we may compare with exact results. The exact solution for the sphere is given by

the coefficients

$$A_\ell = \frac{\kappa a\, j_\ell(ka)\, j_\ell'(\kappa a) - ka\, j_\ell'(ka)\, j_\ell(\kappa a)}{ka\, h_\ell'(ka)\, j_\ell(\kappa a) - \kappa a\, h_\ell(ka)\, j_\ell'(\kappa a)}$$

$$B_\ell = \frac{ka[h_\ell'(ka)\, j_\ell(ka) - h_\ell(ka)\, j_\ell'(ka)]}{ka\, h_\ell'(ka)\, j_\ell(\kappa a) - \kappa a\, h_\ell(ka)\, j_\ell'(\kappa a)} \qquad (7)$$

It is instructive and possible to apply the approximation (5) piecemeal to the sphere. We consider three successive procedures: (1) Exact boundary condition for normal component of the gradient of ψ but approximate boundary condition for ψ; (2) Exact boundary condition on ψ but approximate one for the gradient of ψ; (3) Full approximation as given in Eq. (5). In all cases the coefficients are solved by the same truncation of the series expressions. We denote the solutions obtained by procedures (1), (2) and (3) by $A_{\ell,1}^{(2s)}$, $A_{\ell,2}^{(2s)}$ and $A_\ell^{(2s)}$ etc. respectively.

Procedure (1) involves the simultaneous solution of:

From (5a) and (4)

$$e^{ika\mu_i} + \sum_{\ell=0}^{2s-1} (-1)^\ell (2\ell+1)\, A_{\ell,1}^{(2s)}\, h_\ell(ka)\, P_\ell(\mu_i) = \sum_{\ell=0}^{2s-1} (-1)^\ell (2\ell+1)\, B_{\ell,1}^{(2s)}\, j_\ell(\kappa a)\, P_\ell(\mu_i) \qquad (8a)$$

and from (2b) and (3)

$$ka\,[j_\ell'(ka) + h_\ell'(ka)\, A_\ell] = \kappa a\, B_\ell\, j_\ell'(\kappa a) \qquad (8b)$$

In simultaneously solving for the A's and B's in Eqs. (8a) and (8b), we let the A_ℓ and B_ℓ of Eq. (8b) be equated to the $A_{\ell,1}^{(2s)}$ and $B_{\ell,1}^{(2s)}$ of Eq. (8a).

As a simplification in the numerical analysis the equation (8a) may be separated into two sets of equations, each of which is

either even or odd in μ_i.

The result of combining (8a) and (8b) is

$$A_{\ell,1}^{(2s)}(ka) = \left\{1 + \rho_\ell^{(2s)}(ka)\right\} A_\ell(ka) \tag{9}$$

where

$$\rho_\ell^{(2s)} = \left\{ \frac{\Lambda_\ell^{(2s)}(ka) - 1}{ka\, j_\ell'(ka)\, j_\ell(ka)} \right\} \Bigg/ \left\{ 1 - \left[\frac{}{\kappa a\, j_\ell(ka)\, j_\ell'(\kappa a)} \right] \right\} \tag{10}$$

and $\Lambda_\ell^{(2s)}(ka)$ is a rather complicated algebraic expression which we shall not present here. Instead we give the expansions of $\Lambda_\ell^{(2s)}(ka)$ in powers of ka which, for even and odd values of ℓ are

$$\Lambda_{2\ell}^{(2s)}(ka) = \sum_{n=0}^{s-\ell-1} \frac{(-1)^n (ka)^{2n+2\ell} c_{2n+2\ell,\,2\ell}}{(2n+2\ell)!(4\ell+1)\, j_{2\ell}(ka)} + L^{(2s)}(\mu_i) \tag{11a}$$

and

$$\Lambda_{2\ell+1}^{(2s)}(ka) = \sum_{n=0}^{s-\ell-1} \frac{(-1)^n (ka)^{2n+2\ell+1} c_{2n+2\ell+1,\,2\ell+1}}{(2n+2\ell+1)!(4\ell+3)\, j_{2\ell+1}(ka)} + M^{(2s)}(\mu_i) \tag{11b}$$

where $L^{(2s)}(\mu_i)$ and $M^{(2s)}(\mu_i)$ are functions of the angles at which the B.C.'s are satisfied. Both $L^{(2s)}$ and $M^{(2s)}$ are expansions in (ka) in which the lowest order term is $(ka)^{2s}$ and $(ka)^{2s+1}$ respectively.

The quantities $c_{2n,2}$ and $C_{2n+1,\,2m+1}$ are coefficients in the expansions

$$\mu^{2n} = \sum_{i=0}^{n} c_{2n,2i} P_{2i}(\mu), \quad \mu^{2n+1} = \sum_{i=0}^{n} C_{2n+1,\,2i+1} P_{2i+1}(\mu)$$

Procedure (2) involves the simultaneous solution of:

From (5b) and (4)

$$ika\,\mu_i e^{ika\mu_i} + ka \sum_{\ell+1}^{2s-1} (2\ell+1) i^\ell A_{\ell,2}^{(2s)} h_\ell'(ka) P_\ell(\mu_i) = \kappa a \sum_{\ell=0}^{2s-1} (2\ell+1) i^\ell B_{\ell,2}^{(2s)} j_\ell'(\kappa a) P_\ell(\mu_i) \tag{12a}$$

and from (2a) and (3)

$$[j_\ell(ka) + h_\ell(ka)\, A_\ell] = j_\ell(\kappa a)\, B_\ell \tag{12b}$$

Similarly to our previous treatment we consider the A_ℓ and B_ℓ in (12b) as approximate values $A_{\ell,2}^{(2s)}$ and $B_{\ell,2}^{(2s)}$ and combine (12a) and (12b) to obtain

$$A_{\ell,2}^{(2s)} = [1 + \xi_\ell^{(2s)}(ka)]\, A_\ell \tag{13}$$

where

$$\xi_\ell^{(2s)}(ka) = \frac{\Gamma_\ell^{(2s)}(ka) - 1}{\kappa a\, j_\ell(ka)\, j_\ell'(\kappa a)\Big/\left[1 - \left[\frac{ka\, j_\ell'(ka)\, j_\ell(\kappa a)}{}\right]\right]} \tag{14}$$

The quantities $\Gamma_\ell^{(2s)}(ka)$ when expanded in powers of (ka) are very similar to the $\Lambda_\ell^{(2s)}$ and are given by (for ℓ even and odd respectively)

$$\Gamma_{2\ell}^{(2s)}(ka) = \sum_{n=0}^{s-\ell-1} \left[\frac{(-1)^n (ka)^{2n+2\ell-1} c_{2n+2\ell,\,2\ell}}{(2n+2\ell-1)!\,(4\ell+1)\, j_{2\ell}'(ka)}\right] + N^{(2s)}(\mu_i) \tag{15a}$$

$$\Gamma_{2\ell+1}^{(2s)}(ka) = \sum_{n=0}^{s-\ell-1} \frac{(-1)^n (ka)^{2n+2\ell} c_{2n+2\ell+1,\,2\ell+1}}{(2n+2\ell)!\,(4\ell+3)\, j_{2\ell+1}'(ka)} + 0^{(2s)}(\mu_i) \tag{15b}$$

where only the functions of the higher powers of (ka) involve the choice of B.C. angles μ_i.

Finally then we use the full approximation to obtain from Eq. (8a) and (12a) the coefficients

$$A_\ell^{(2s)} = \frac{\kappa a\, j_\ell(ka)\, j_\ell'(\kappa a)\, \Lambda_\ell^{(2s)}(ka) - ka\, j_\ell'(ka)\, j_\ell(\kappa a)\, \Gamma_\ell^{(2s)}(ka)}{ka\, h_\ell'(ka)\, j_\ell(\kappa a) - \kappa a\, h_\ell(ka)\, j_\ell'(\kappa a)} \tag{16a}$$

$$B_\ell^{(2s)} = \frac{ka\,[h_\ell'(ka)\, j_\ell(ka)\, \Lambda_\ell^{(2s)}(ka) - h_\ell(ka)\, j_\ell'(ka)\, \Gamma_\ell^{(2s)}(ka)]}{ka\, h_\ell'(ka)\, j_\ell(\kappa a) - \kappa a\, h_\ell(ka)\, j_\ell'(\kappa a)} \tag{16b}$$

where the modifying coefficients $\Lambda_\ell^{(2s)}$ and $\Gamma_\ell^{(2s)}$ are identical to those defined by equations (11) and (15).

We may then write

$$A_\ell^{(2s)} = [1 + \rho_\ell^{(2s)}(ka) + \xi_\ell^{(2s)}(\kappa a)]\, A_\ell \qquad (17)$$

Several general facts are rather evident. It can be seen by tracing back along the trail of definitions of ρ_ℓ and ξ_ℓ that both of these quantities are real (for real κ) and that consequently the phases of the exact and approximate A_ℓ are identical. Further we see that the approximation is independent of the choice of angles up to some power of (ka) [at least $(ka)^{2s}$]. This means that for $\ell = 2s - 1$ we obtain only the leading term in the expansion (in ascending powers of ka) but that for smaller values of ℓ we obtain successively more and more terms which are independent of the choice of boundary points. Finally as $ka \to 0$ the $A_\ell^{(2)}$ go as $(ka)^{2\ell+1}$ and become identical with the Rayleigh approximation.

The approximate expressions are so complicated that it is certainly not easy to draw any more general inferences if indeed they exist. At this point we must resort to demonstrating the two features which imply the usefulness of our approximation: (1) The values of the coefficients converge reasonably rapidly to some value; and (2) this value is the correct one.

Extensive numerical analysis was carried out in evaluating the quantities A_ℓ, B_ℓ, $\rho_\ell^{(2s)}$ and $\xi_\ell^{(2s)}$. We present in Tables 1 and 2 some sets of values of $\rho_\ell^{(2s)}$ (partial procedure (1)) and $\rho_\ell^{(2s)} + \xi_\ell^{(2s)}$ (full approximation procedure) for spheres with refractive index m = 1.3.

Noting that the validity of the approximation is justified only if the quantities $\rho_\ell^{(2s)}$ and $\xi_\ell^{(2s)}$ are small it is rather interesting to

Table 1

Numerical Values of the $\rho_{\ell}^{(2s)}$ (ka) for the Refractive Index m = 1.3

s = 2

$\rho_i^{(4)}$ ka	ka = 0.2	ka = 0.4	ka = 0.6	ka = 0.8	ka = 1.0	ka = 1.5	ka = 2.0
0	2.2(-5)	3.5(-4)	1.8(-3)	5.9(-3)	1.4(-2)	7.6(-2)	2.5(-1)
1	-1.7(-4)	-1.3(-3)	-1.3(-3)	-2.1(-3)	-2.7(-3)	-1.3(-3)	1.0(-1)
2	2.4(-1)	2.3(-1)	2.4(-1)	2.1(-1)	2.0(-1)	1.8(-1)	9.2(-1)
3	1.9(-1)	2.6(-1)	2.5(-1)	2.6(-1)	2.5(-1)	2.2(-1)	1.9(-1)

s = 3

$\rho_i^{(6)}$ ka	ka = 0.2	ka = 0.4	ka = 0.6	ka = 0.8	ka = 1.0	ka = 1.5	ka = 2.0
0	2.1(-9)	1.3(-7)	1.6(-6)	8.9(-6)	3.5(-5)	4.3(-4)	2.7(-3)
1	1.1(-7)	1.7(-6)	8.1(-6)	2.3(-5)	4.6(-5)	4.9(-5)	-7.7(-4)
2	-1.6(-4)	-6.3(-4)	-1.4(-3)	-2.4(-3)	-3.5(-3)	-6.3(-3)	-7.0(-3)
3	-1.3(-4)	-5.4(-4)	-1.2(-3)	-2.1(-3)	-3.2(-3)	-6.5(-3)	-9.7(-3)
4	2.9(-1)	2.9(-1)	2.8(-1)	2.8(-1)	2.8(-1)	2.6(-1)	2.3(-1)
5	-1.6	-7.3(-1)	-7.2(-1)	-7.2(-1)	-7.1(-1)	-6.9(-1)	-6.5(-1)

s = 4

$\rho_i^{(8)}$ ka	ka = 0.2	ka = 0.4	ka = 0.6	ka = 0.8	ka = 1.0	ka = 1.5	ka = 2.0
0	-6.1(-13)	-1.6(-11)	-4.1(-10)	-4.2(-9)	-2.5(-8)	-6.9(-7)	-7.2(-6)
1	3.6(-12)	1.5(-10)	1.5(-9)	7.7(-9)	2.4(-8)	6.0(-8)	-1.7(-6)
2	-1.3(-8)	-2.0(-7)	-9.8(-7)	-3.0(-6)	-7.0(-6)	-2.9(-5)	-5.8(-5)
3	6.2(-7)	3.7(-7)	1.9(-6)	5.9(-6)	1.4(-5)	6.5(-5)	1.8(-4)
4	-4.3(-3)	-4.4(-5)	-9.6(-4)	-1.7(-3)	-2.6(-3)	-5.5(-3)	-9.0(-3)
5	-1.5(-2)	-6.4(-3)	5.5(-4)	1.7(-3)	2.7(-3)	5.8(-3)	9.8(-3)
6	3.1(-1)	3.1(-1)	3.1(-1)	3.1(-1)	3.0(-1)	2.9(-1)	2.8(-1)
7	9.2(-1)	9.1(-1)	9.1(-1)	9.1(-1)	9.0(-1)	8.8(-1)	8.5(-1)

Table 2

Numerical Values of the $\tau_{\ell}^{(2s)}(ka) = \rho_{\ell}^{(2s)}(ka) + \zeta_{\ell}^{(2s)}(ka)$ for m = 1.3

s = 2

$\tau_i^{(4)}$ka	ka = 0.2	ka = 0.4	ka = 0.6	ka = 0.8	ka = 1.0	ka = 1.5	ka = 2.0
0	-9.0(-4)	-3.6(-3)	-4.2(-2)	-9.0(-3)	-8.4(-3)	4.3(-2)	2.2(-1)
1	5.6(-4)	2.2(-3)	7.6(-2)	1.5(-2)	1.8(-2)	4.2(-2)	-7.6(-2)
2	-1.1	-7.5(-1)	-1.1	-1.1	-1.1	-1.0	-9.8(-1)
3	1.1	-1.7(-1)	-1.9(-1)	-1.9(-1)	-2.1(-1)	-2.0(-1)	-2.1(-1)

s = 3

$\tau_i^{(6)}$ka	ka = 0.2	ka = 0.4	ka = 0.6	ka = 0.8	ka = 1.0	ka = 1.5	ka = 2.0
0	-1.4(-6)	-2.2(-5)	-1.1(-4)	-3.3(-4)	-7.6(-4)	-3.0(-3)	-4.1(-3)
1	-6.8(-7)	-1.1(-5)	-5.6(-5)	-1.8(-4)	-4.5(-4)	-2.4(-3)	-9.9(-3)
2	5.6(-4)	1.5(-3)	5.1(-3)	9.1(-3)	1.4(-2)	3.2(-2)	5.9(-2)
3	1.8(-4)	7.3(-3)	1.6(-3)	2.9(-3)	4.7(-3)	1.1(-2)	2.0(-2)
4	6.4(-1)	6.5(-1)	6.5(-1)	6.4(-1)	6.4(-1)	6.1(-1)	5.8(-1)
5	-18.7	2.8(-1)	3.0(-1)	3.0(-1)	3.0(-1)	3.2(-1)	3.4(-1)

s = 4

$\tau_i^{(8)}$ka	ka = 0.2	ka = 0.4	ka = 0.6	ka = 0.8	ka = 1.0	ka = 1.5	ka = 2.0
0	-2.2(-11)	-1.4(-9)	-1.6(-8)	-8.9(-8)	-3.4(-7)	-2.4(-6)	-1.7(-5)
1	-2.0(-11)	-1.2(-9)	-1.4(-8)	-8.1(-8)	-3.1(-7)	-3.2(-6)	2.4(-5)
2	3.8(-8)	4.1(-7)	3.1(-6)	10.0(-5)	2.5(-5)	1.3(-4)	4.4(-4)
3	-1.6(-6)	-8.0(-6)	-3.9(-6)	-1.3(-5)	-3.1(-5)	-1.6(-4)	-5.3(-4)
4	-9.2(-3)	8.1(-4)	9.8(-3)	1.8(-3)	3.0(-3)	6.4(-2)	1.2(-2)
5	-2.0(-1)	-1.5(-2)	-1.7(-3)	-1.4(-3)	-2.2(-3)	-5.2(-3)	-9.6(-3)
6	-1.0(-1)	-1.0(-1)	-1.1(-1)	-1.0(-1)	-1.1(-1)	-1.1(-1)	-1.1(-1)
7	-2.6(-1)	-2.6(-1)	-2.6(-1)	-1.2(-1)	-2.7(-1)	-2.8(-1)	-2.9(-1)

observe the numerically experimental fact that the full approximation procedure is not consistently worse and is in many cases better than procedure (1) in which the B.C.'s are presumably better satisfied.

We have explicitly evaluated the $\rho_\ell^{(2s)}$ and $\xi_\ell^{(2s)}$ only for values of ka up to ka = 2 (implicitly they were calculated up to ka = 5.8). In any case it is clear to see that for s = 2, the first two scattering coefficients $A_\ell^{(2s)}$ are good to within a few percent up to ka = 2. For s = 3 we obtain the first four scattering coefficients to this order of accuracy; and finally for s = 4, the first six are so defined. Although one would expect the values of $\rho_\ell^{(2s)}$ to be consistently smaller for smaller values of ka than for larger values of ka, we have found this not to be true. For example, the value of $\rho_3^{(4)}$ is largest for ka = 0.2 and is almost constant from ka = 0.4 to ka = 2.0. It should be pointed out that for smaller values of ka it is possible that numerical errors may have accumulated in the inversion of the simultaneous equation matrix so that the value of $\rho_3^{(4)}$ might be in error. In general, the computational procedure of inverting the matrices is such that if ka is small, it is preferable to use an approximation whose order is not much larger than the minimum one required.

Tables 3 and 4 are to be compared term by term for differences in the complex scattering coefficients which show up as dependent on varying the selection of angles at which the B.C.'s are satisfied. Several conclusions are evident after a careful perusal of these two tables. One conclusion is that over the expected range of validity of

Table 3

Scattering Coefficients $A_\ell^{(8)}$ for a Sphere of Refractive Index m = 1.3

Angular Positions at which Boundary Conditions are Satisfied are

$\theta_1 = 10^\circ$, $\theta_2 = 32.5^\circ$, $\theta_3 = 55^\circ$, $\theta_4 = 77.5^\circ$

ka	$A_0^{(8)}$	$A_1^{(8)}$	$A_2^{(8)}$	$A_3^{(8)}$
1.0	-0.049,534,84 i0.216,981,8	-2.095,560(-4) i0.014,475,2	-1.646,739(-7) i4.057,968(-4)	-4.873,225(-11) i6.470,687(-6)
2.0	-0.423,076,0 i0.494,041,9	-0.146,019,9 i0.353,127,0	-1.927,607(-3) i0.043,859,41	-7.381,245(-6) i2.716,772(-3)
3.0	-0.486,047,5 i0.499,869,7	-0.665,144,1 i0.471,970,6	-0.299,405,8 i0.457,759,2	-6,855,142(-3) i0.082,501,63
4.0	-0.939,155,5 i0.244,630,7	-0.716,439,4 i0.450,687,1	-0.838,190,8 i0.365,549,5	-0.508,918,1 i0.499,542,4
5.0	-0.991,155,4 i0.119,272,8	-0.996,484,7 i0.014,720,876	-0.877,347,5 i0.328,293,3	-0.945,681,7 i0.223,482,4

ka	$A_4^{(8)}$	$A_5^{(8)}$	$A_6^{(8)}$	$A_7^{(8)}$
1.0	-1.003,705(-13) i6.583,169(-8)	5.244,207(-14) i4.640,630(-10)	2.691,890(-18) i2.028,563(-12)	1.154,230(-18) i8.836,961(-15)
2.0	-1.245,258(-8) i1.115,763(-4)	-1.026,259(-11) i3.211,343(-6)	-3.745,451(-15) i5.585,579(-8)	-2.406,651(-18) i1.117,888(-9)
3.0	-5.298,698(-5) i7.274,703(-3)	-2.252,085(-7) i4.776,254(-4)	-4.164,604(-10) i1.837,003(-5)	-7.261,956(-13) i8.727,847(-7)
4.0	-0.017,535,81 i0.130,993,5	-2.056,689(-4) i0.014,530,29	-1.121,423(-6) i9.316,697(-4)	-6.749,310(-9) i8.438,223(-5)
5.0	-0.730,802,8 i0.434,599,0	-0.040,915,22 i0.203,205,4	-3.996,412(-4) i0.016,984,88	-6.097,832(-6) i2.545,918(-3)

Table 4

Scattering Coefficients $A_\ell^{(8)}$ for a Sphere of Refractive Index m = 1.3

Angular Positions at which Boundary Conditions are Satisfied are

$\theta_1 = 0^\circ$, $\theta_2 = 22.5^\circ$, $\theta_3 = 45^\circ$, $\theta_4 = 67.5^\circ$

ka	$A_0^{(8)}$	$A_1^{(8)}$	$A_2^{(8)}$	$A_3^{(8)}$
1.0	-0.049,534,32 i0.216,979,5	-2.095,557(-4) i0.014,474,52	-1.646,443(-7) i4.057,418(-4)	-4.429,208(-11) i6.470,727(-6)
2.0	-0.422,831,5 i0.493,756,3	-0.146,019,17 i0,353,125,1	-1.923,037(-3) i0.043,755,42	-7,381,756(-6) i2.716,960(-3)
3.0	-0.488,770,3 i0,502,669,9	-0.665,107,3 i0,471,944,5	-0.295,333,8 i0.451,533,5	-6.857,578(-3) i0,082,530,94
4.0	-1.045,818 i0.272,414,2	-0.716,441,3 i0.450,744,9	-0.801,279,1 i0.349,451,7	-0.509,469,7 i0.500,083,8
5.0	-1.197,145 i0.144,061,1	-1.000,568 i0.014,781,20	-0.878,284,0 i0.328,643,7	-0.947,674,3 i0.223,953,35

ka	$A_4^{(8)}$	$A_5^{(8)}$	$A_6^{(8)}$	$A_7^{(8)}$
1.0	-2.162,455(-15) i6.536,006(-8)	1.849,599(-13) i2.604,276(-11)	-4.208,555(-19) i1.173,327(-12)	-7.256,898(-19) i2.497,293(-16)
2.0	-1.207,444(-8) i1.081,871(-4)	-1.014,600(-11) i3.185,952(-6)	-2.072,432(-15) i3.122,903(-8)	9.036,006(-18) i7.667,151(-10)
3.0	-4.897,194(-5) i6.723,468(-3)	-2.207,244(-7) i4.681,155(-4)	-2.122,014(-10) i9.360,192(-6)	-4.769,251(-13) i5.732,091(-7)
4.0	-0.014,826,46 i0.110,754,5	-1.972,147(-4) i0.013,933,01	-4.864,164(-7) i4,041,107(-4)	-4.148,749(-9) i5.186,912(-5)
5.0	-0.525,503,7 i0.312,510,3	-0.037,784,93 i0.187,658,8	-1.290,071(-4) i5.482,845(-3)	-3.406,539(-6) i1.422,271(-3)

the approximation ($\ell \lesssim s$, $ka \lesssim s$) the differences in these scattering coefficients is trivial except where the coefficients themselves become so small as to be negligible. As has already been pointed out the phases of the scattering coefficients should be and are invariant to the choice of angles. The tables have been spot checked for this as an indication of the possibility of numerical error and no deviations have been detected.

Tables 5 and 6 indicate again how the important terms in the series are independent of the choice of B.C. angles. In particular we see that for s = 6 the values of the scattering coefficients for sizes up to ka = 5 are given within better than one percent up to ℓ = 7 (8th term) where the coefficients may already be neglected.

For calculating the total cross-section for a given value of ka it appears from Table 7 that one can be guaranteed of an accuracy considerably better than one percent by using the approximation which involves a number of B.C. points equal to the nearest integer less than ka.

c. Approximate scattering by prolate spheroids

The configuration appropriate to this problem is shown in Fig. 1. We consider a prolate spheroid of length 2b and width 2a ($b \geq a$) whose symmetry axis is along the direction of propagation of the scalar radiation.

The equation for the surface of the spheroid is

$$\frac{r}{a} = (1 - \eta^2 \cos^2\theta)^{-\frac{1}{2}} \tag{18}$$

where $\eta^2 = 1 - (a/b)^2$. Although there might be some advantage in using speroidal coordinates we have found it easier, at least in this first approach, to continue to use spheroidal coordinates. The expansions for the interior and exterior wave functions are then formally exactly the same as they were for the sphere and the

Table 5

Table 6

Scattering Coefficients for a Sphere of Refractive Index m = 1.3

Angular Positions at which Boundary Conditions are Satisfied are
$\theta_1 = 8^\circ$, $\theta_2 = 22^\circ$, $\theta_3 = 36^\circ$, $\theta_4 = 50^\circ$
$\theta_5 = 64^\circ$, $\theta_6 = 78^\circ$

	ka = 4	ka = 5
$A_0^{(12)}$	-0.936,519,3 i0.243,944,0	-0.985,896,9 i0.118,640,0
$A_1^{(12)}$	-0.716,423,2 i0.450,733,6	-0.999,776,7 i0.014,769,50
$A_2^{(12)}$	-0.840,176,5 i0.366,415,5	-0.877,252,7 i0.328,357,8
$A_3^{(12)}$	-0.509,296,1 i0.499,913,4	-0.947,106,47 i0.223,819,1
$A_4^{(12)}$	-0.017,603,28 i0.131,497,4	-0.738,400,7 i0.439,114
$A_5^{(12)}$	-2.003,107(-4) i0.014,151,74	-0.038,962,97 i0.193,509,6
$A_6^{(12)}$	-1.447,620(-6) i1.202,670(-3)	-5.520,048(-4) i0.023,460,39
$A_7^{(12)}$	-6.398,064(-9) i7.998,417(-5)	-5.736,642(-6) i2.395,116(-3)
$A_8^{(12)}$	-1.762,039(-11) i4.155,607(-6)	-3.896,484(-8) i1.957,383,6(-4)
$A_9^{(12)}$	-3.913,989(-14) i1 776,048(-7)	-1.811,698(-10) i1.349,351(-5)
$A_{10}^{(12)}$	-9.873,709(-17) i5.030,706(-9)	-4.395,214(-13) i5.904,508(-7)
$A_{11}^{(12)}$	-1.009,969(-17) i1.748,354(-10)	-1.114,085(-15) i3.368,192(-3)

Angular Positions at which Boundary Conditions are Satisfied are
$\theta_1 = 0^\circ$, $\theta_2 = 15^\circ$, $\theta_3 = 30^\circ$, $\theta_4 = 45^\circ$
$\theta_5 = 60^\circ$, $\theta_6 = 75^\circ$

	ka = 4	ka = 5
$A_0^{(12)}$	-0.936,698,8 i0.243,990.8	-0.986,421,9 i0.118,703,2
$A_1^{(12)}$	-0.716,423,4 i0.450,733,7	-0.999,782,7 i0.014,769,59
$A_2^{(12)}$	-0.840,119,5 i0.366,390,7	-0.877,455,1 i0.328,333,5
$A_3^{(12)}$	-0.509,296,3 i0.499,913,6	-0.947,107,9 i0.223,819,5
$A_4^{(12)}$	-0.017,597,82 i0.131,456,7	-0.737,409,0 i0.438,527,6
$A_5^{(12)}$	-2.003,091(-4) i0.014,151,63	-0.038,961,65 i0.193,502,9
$A_6^{(12)}$	-1.444,638(-6) i1.200,190(-3)	-5.488,371(-4) i0.032,235,76
$A_7^{(12)}$	-6.401,423(-9) i7.998,753(-5)	-5.737,106(-6) i2.395,310(-3)
$A_8^{(12)}$	-1.707,119(-11) i4.056,325(-6)	-3.735,678(-8) i1.876,609(-4)
$A_9^{(12)}$	-1.499,002(-13) i1.764,777(-7)	-1.790,520(-10) i1.334,291(-5)
$A_{10}^{(12)}$	-6.721,264(-17) i3.735,586(-9)	-3.131,437(-13) i4.209,051(-7)
$A_{11}^{(12)}$	-9.904,413(-17) i1.393,141(-10)	-8.466,696(-16) i2.613,487(-8)

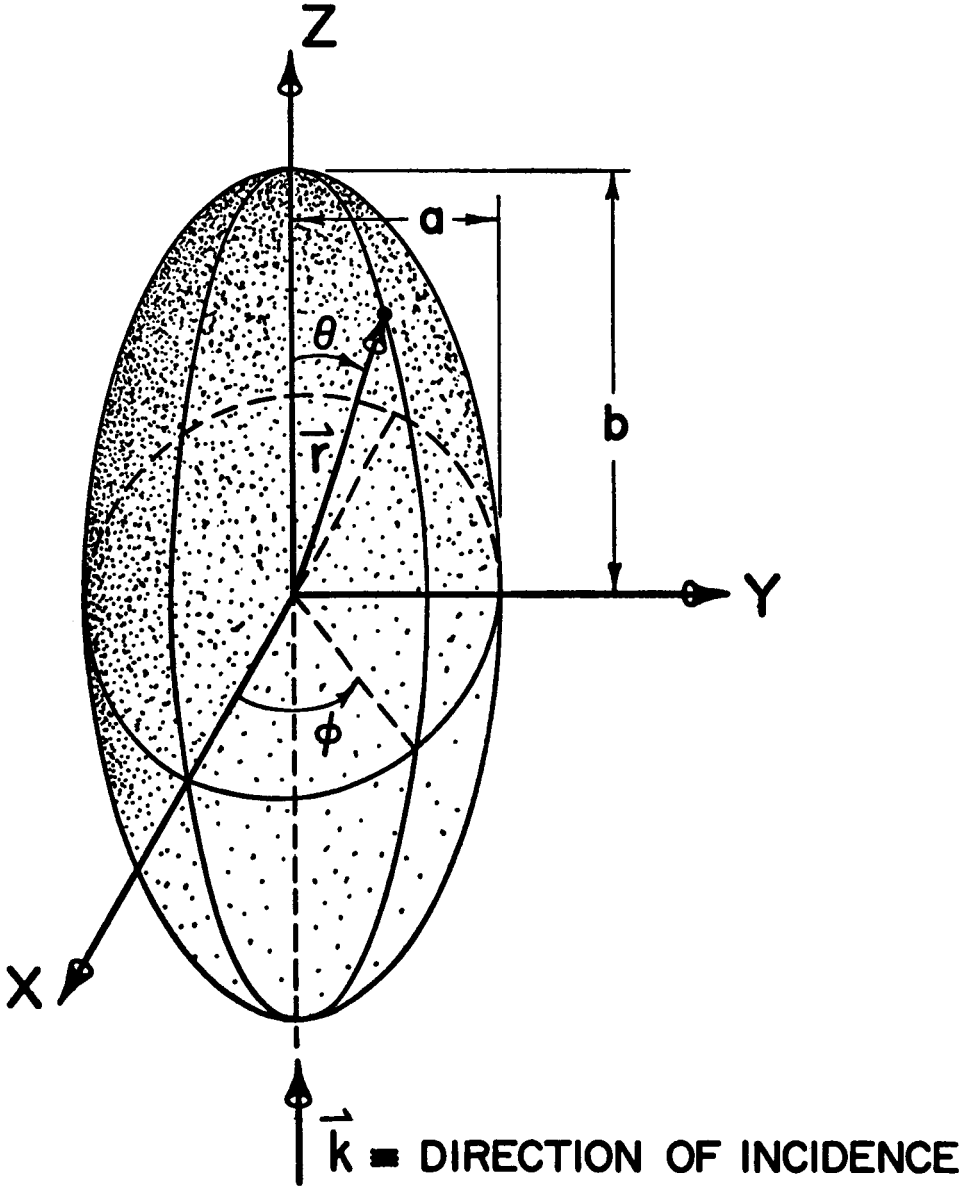

Figure 1 ORIENTATION OF SPHEROID SCATTERER AND DIRECTION OF INCIDENCE OF SCALAR PLANE WAVE

Table 7

Exact and Approximate Scattering Efficiency Factors

for a Sphere with Refractive Index m = 1.3

	ka = 0.4	ka = 0.8	ka = 1.0	ka = 1.4	ka = 1.8	ka = 2.0
Q	5.527,85(-3)	0.088,425	0.200,655	0.487,09	0.703,52	0.870,83
$Q^{(8)}$	5.530,11(-3)	0.088,488	0.200,658	0.487,272	0.703,522	0.870,826
$Q^{(10)}$	5.528,50(-3)	0.088,488	0.200,658	0.487,273	0.703,524	0.870,829
$Q^{(12)}$		0.088,488	0.200,657	0.487,273	0.703,524	0.870,831

	ka = 2.4	ka = 2.8	ka = 3.0	ka = 3.2	ka = 3.6	ka = 4.0
Q	1.273,64	1.573,81	1.790,19		2.340,13	2.753,11
$Q^{(8)}$	1.273,626	1.573,636	1.789,767	2.019,190	2,338,452	2.750,422
$Q^{(10)}$	1.273,637	1.573,762	1.790,077	2.019,776	2.339,667	2.752,484
$Q^{(12)}$	1.273,643	1.573,807	1.790,189	2.020,001	2,340,117	2.753,100

	ka = 4.6	ka = 5.0	ka = 5.4	ka = 5.8
Q		3.533,64		
$Q^{(8)}$	3.175,907	3.523,152	3.663,221	3.990,987
$Q^{(10)}$	3.178,406	3.521,577	3.642,263	3.924,411
$Q^{12)}$	3.182,225	3.533,232	3.656,848	3.937,768

equations defining the approximate wave functions are the same as Eq. (4).

The boundary conditions (Eqs. (2) or (5)) are to be applied now at the surface defined by Eq. (18). Applying the boundary conditions we get the resulting sets of equations for matching the function:

$$e^{i\rho\mu} + \sum_{\ell=0}^{2s-1} i^{\ell}(2\ell+1)\, h_{\ell}(\rho)\, A_{\ell}^{(2s)}\, P_{\ell}(\mu) = \sum_{\ell=0}^{2s-1} i^{\ell}(2\ell+1)\, j_{\ell}(\xi)\, B_{\ell}^{(2s)}\, P_{\ell}(\mu) \tag{19a}$$

and for matching the gradient:

$$\begin{aligned} i\rho\mu\,(1-\eta^2)\, e^{i\rho\mu} + (\alpha^2/\rho) \sum_{\ell=0}^{2s-1} i^{\ell}\,(2\ell+1)\, h_{\ell}'(\rho)\, P_{\ell}(\mu)\, A_{\ell}^{(2s)} \\ - \eta^2\mu\,(1-\mu^2) \sum_{\ell=0}^{2s-1} (2\ell+1)\, h_{\ell}(\rho)\, P_{\ell}'(\mu)\, A_{\ell}^{(2s)} = \\ = (\beta^2/\xi) \sum_{\ell=0}^{2s-1} i^{\ell}(2\ell+1)\, j_{\ell}'(\xi)\, P_{\ell}(\mu)\, B_{\ell}^{(2s)} \\ - \eta^2\mu\,(1-\mu^2) \sum_{\ell=0}^{2s-1} i^{\ell}\,(2\ell+1)\, j_{\ell}(\xi)\, P_{\ell}'(\mu)\, B_{\ell}^{(2s)} \end{aligned} \tag{19b}$$

where

$$\rho = \frac{\alpha}{\sqrt{1-\eta^2\mu^2}}\,, \qquad \xi = \frac{\beta}{\sqrt{1-\eta^2\mu^2}}$$

$$\alpha = ka \qquad \beta = \kappa a \qquad \mu = \cos\theta$$

Equations (19a) and (19b) may be separated into equations which are even and odd in μ and which involve respectively the even and odd values of ℓ.

The expressions become so formidable that little can be deduced from them. We therefore go immediately to a presentation of some numerical results.

Table 8 is presented to show how, (by comparison with Table 7)

Table 8

Scattering Efficiency Factors for a Prolate Spheroid with b/a = 2 and m = 1.3

	ka = 0.4	ka = 0.8	ka = 1.0	ka = 1.4	ka = 1.8	ka = 2.0
$Q^{(8)}$	0.011,920,8	0.236,553	0.484,639	1.758,542	3.193,689	3.450,687
$Q^{(10)}$	0.011,920,8	0.236,554	0.483,859	1.758,101	3.196,556	3.450,397
$Q^{(12)}$			0.484,743	1.759,671	3.194,680	3.450,037
$Q^{(14)}$						3.450,548

	ka = 2.4	ka = 2.8	ka = 3.0	ka = 3.2	ka = 3.6	ka = 4.0
$Q^{(8)}$	4.854,463	5.171,704	4.650,036	5.525,259	6.930,284	7.298,593
$Q^{(10)}$	4.796,134	5.184,812		6.152,740	5.922,495	6.288,430
$Q^{(12)}$	4.798,951	5.138,471		6.268,150	6.061,440	6.261,153
$Q^{(14)}$	4.799,104	5.139,032		6.273,697	6.071,912	6.265,153
$Q^{(16)}$	4.798,918	5.139,445		6.272,457	6.071,789	6.265,833

	ka = 4.5	ka = 5.0	ka = 5.4	ka = 5.8
$Q^{(8)}$	5.262,951	4.222,431	2.752,570	1.447,217
$Q^{(10)}$	5.544,403	4.305,276	2.919,845	2.334,681
$Q^{(12)}$	5.186,779		2.873,365	2.059,084
$Q^{(14)}$	5.373,065		3.260,315	2.206,513
$Q^{(16)}$	5.420,588		3.290,666	2.189,633

the range of validity of the approximation depends on the degree of elongation. It is to be expected that the number of scattering coefficients required to give a certain degree of accuracy should be $\ell \sim (\frac{b}{a})ka$ if it is $\ell \sim ka$ for the sphere. The reason for this is clear when one notes that the phase shift for a ray parallel to the axis of the spheroid is exactly b/a times as large as that for a ray traversing a sphere of radius a. One may reasonably conclude that the order of approximation required for an accuracy of one percent is obtained when s is one less than the nearest integer to (b/a)ka.

Figures 2 and 3 contain a graphic portrayal of differences between various orders of approximation for two elongations (b/a = 1.5 and b/a = 2). Here we have plotted the total scattering efficiency versus the parameter $\rho = 2ka(m-1)$ which is the phase shift of a ray traversing the spheroid along its symmetry axis. The extra points are shown only for ρ values greater than those for which they would fall on the curves. For example we see in Figure 2 that the eight point (s = 4) approximation is acceptable on the m = 1.5 curve up to about $\rho = 3$ (perhaps slightly less) whereas on the m = 1.3 curve, it is acceptable only to about $\rho = 2.2$. Note that this is reasonable because the corresponding values of ka are both about ka = 3. Furthermore in both cases the value of (b/a)ka is greater than four which is the required number of approximating points. We could apply this argument to the results for b/a = 2 presented in Figure 4. We should expect, for example that for s = 5 the approximation should be good for ka = 2.5 or $\rho = 2.5$ and $\rho = 1.5$ for m = 1.5 and 1.3 respectively. It

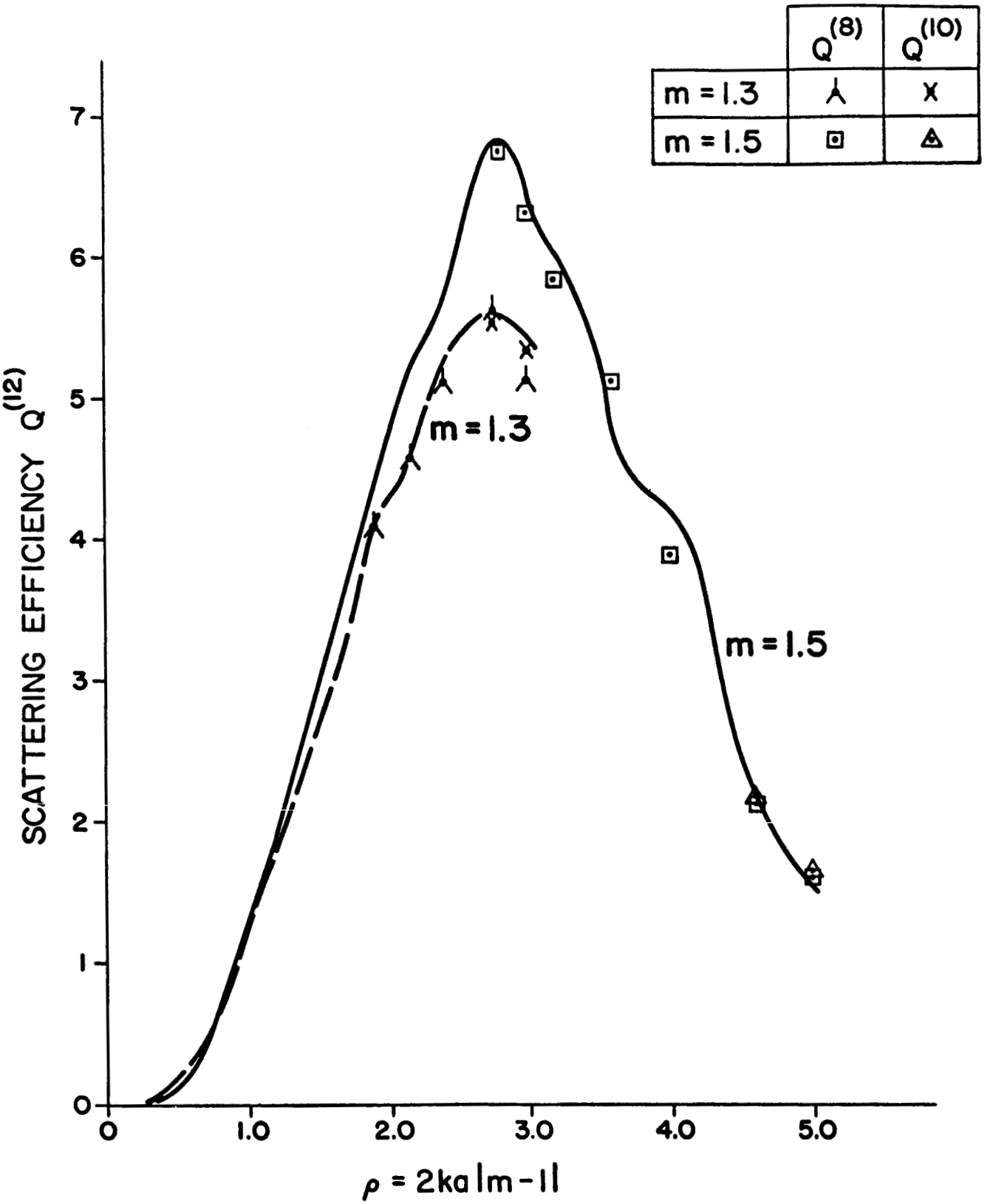

Figure 2 SCATTERING EFFICIENCIES FOR b/a = 1.5, s = 6 AND A SAMPLING OF s = 4 AND 5

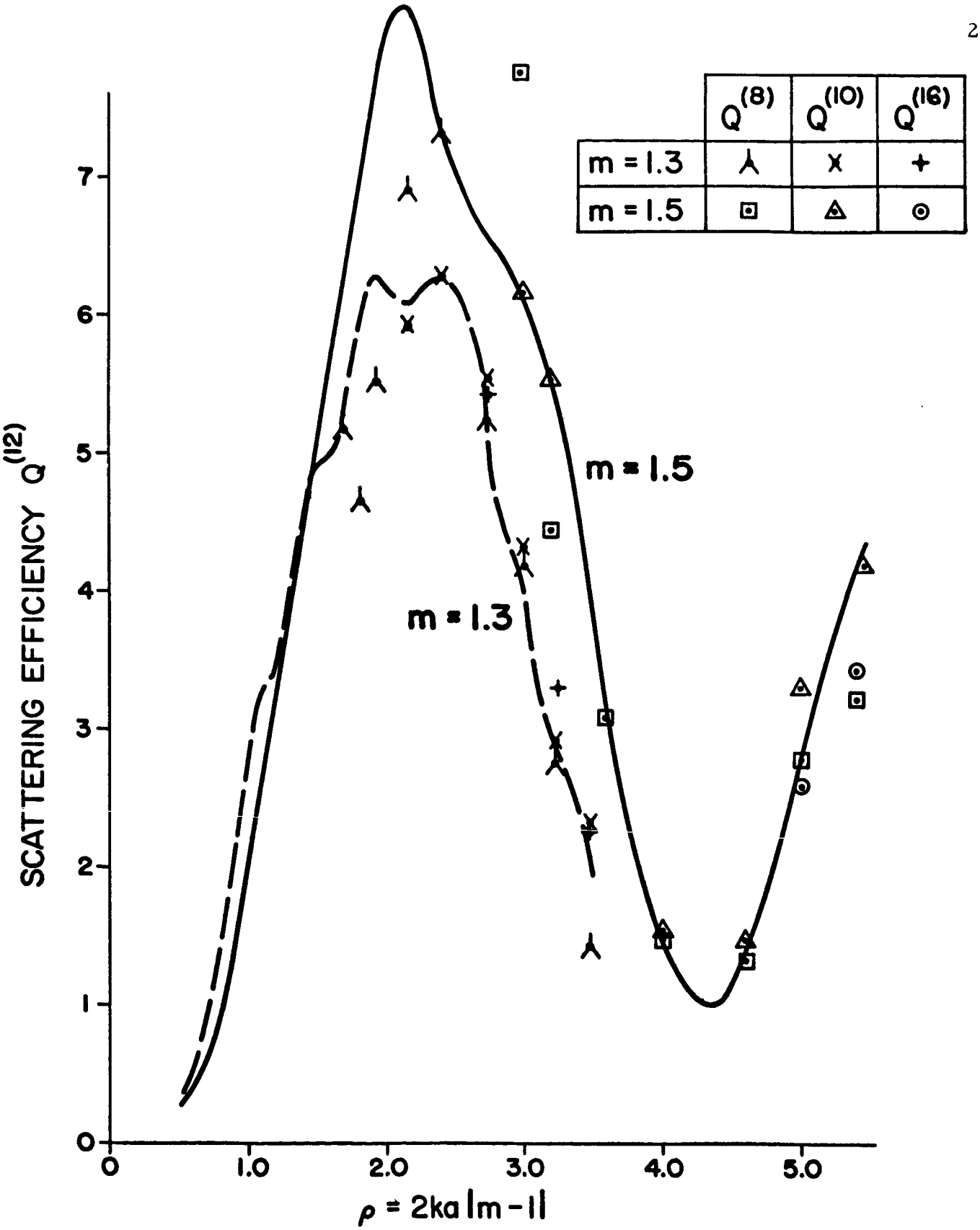

Figure 3 SCATTERING EFFICIENCIES FOR b/a = 2.0, s = 6 AND A SAMPLING OF s = 4,5, AND 8

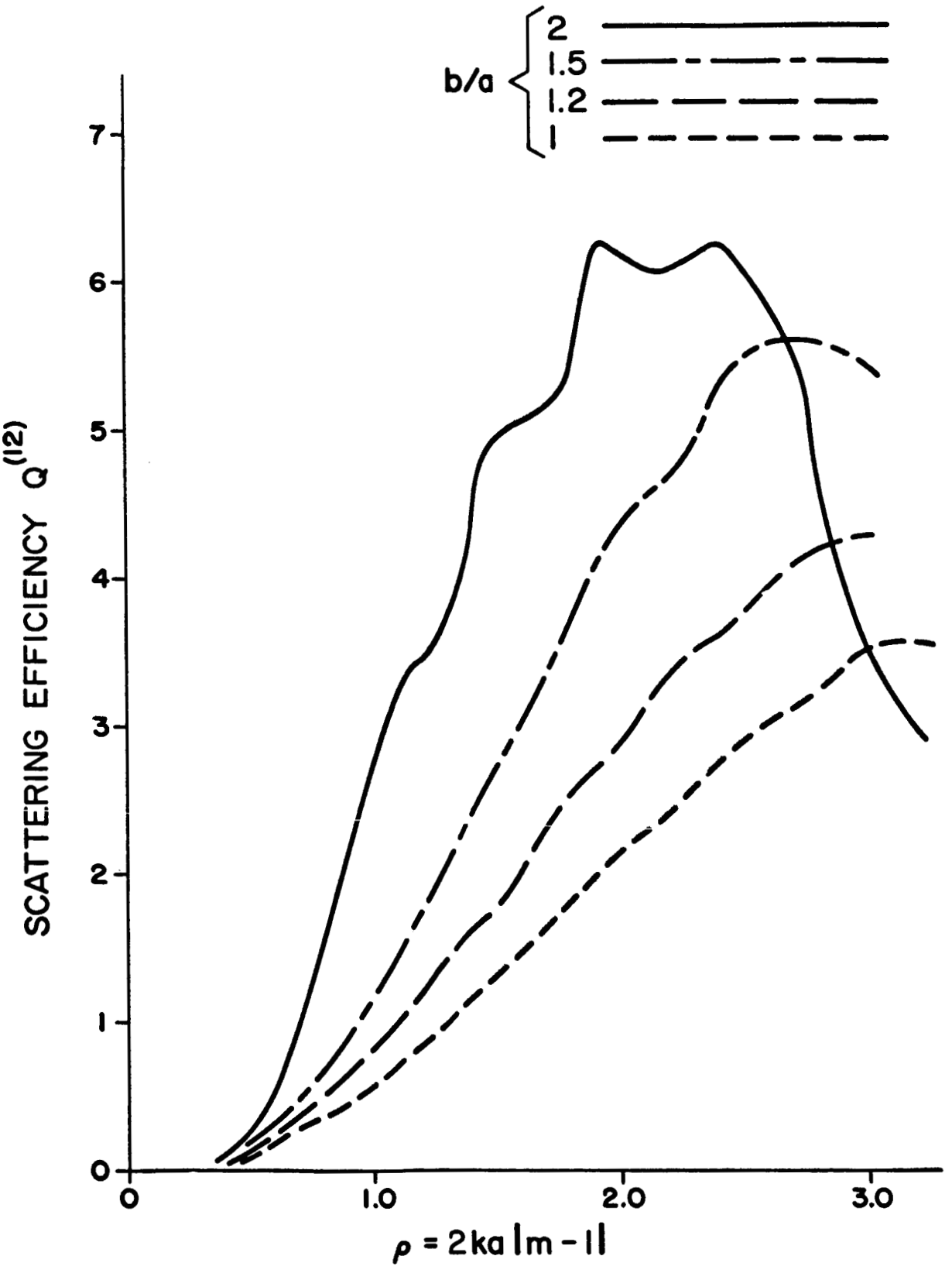

Figure 4 SCATTERING EFFICIENCIES FOR $m = 1.3$, $s = 6$

can be seen that actually the approximation appears to be good up to and somewhat beyond $\rho = 3$ and $\rho = 2$ for the two indices of refraction.

In Figures 4 and 5 we show the effect of elongation on the variation of extinction efficiency with ρ. The shift of the maximum in the total cross-section curves toward shorter values of ρ (by the factor a/b) with increasing b/a has an obvious explanation in terms of a ray approximation.[6] However the interesting result which is lost in the simple ray approximation is the tendency toward increasing the height of the first broad maximum in the efficiency curve as b/a increases, and simultaneously introducing a deeper dip in the first minimum. It should be remarked that this confirms at least these qualitative aspects of early experimental data on scattering by dielectric spheroids.[7] So far no simple theoretical explanation has been given for these effects.

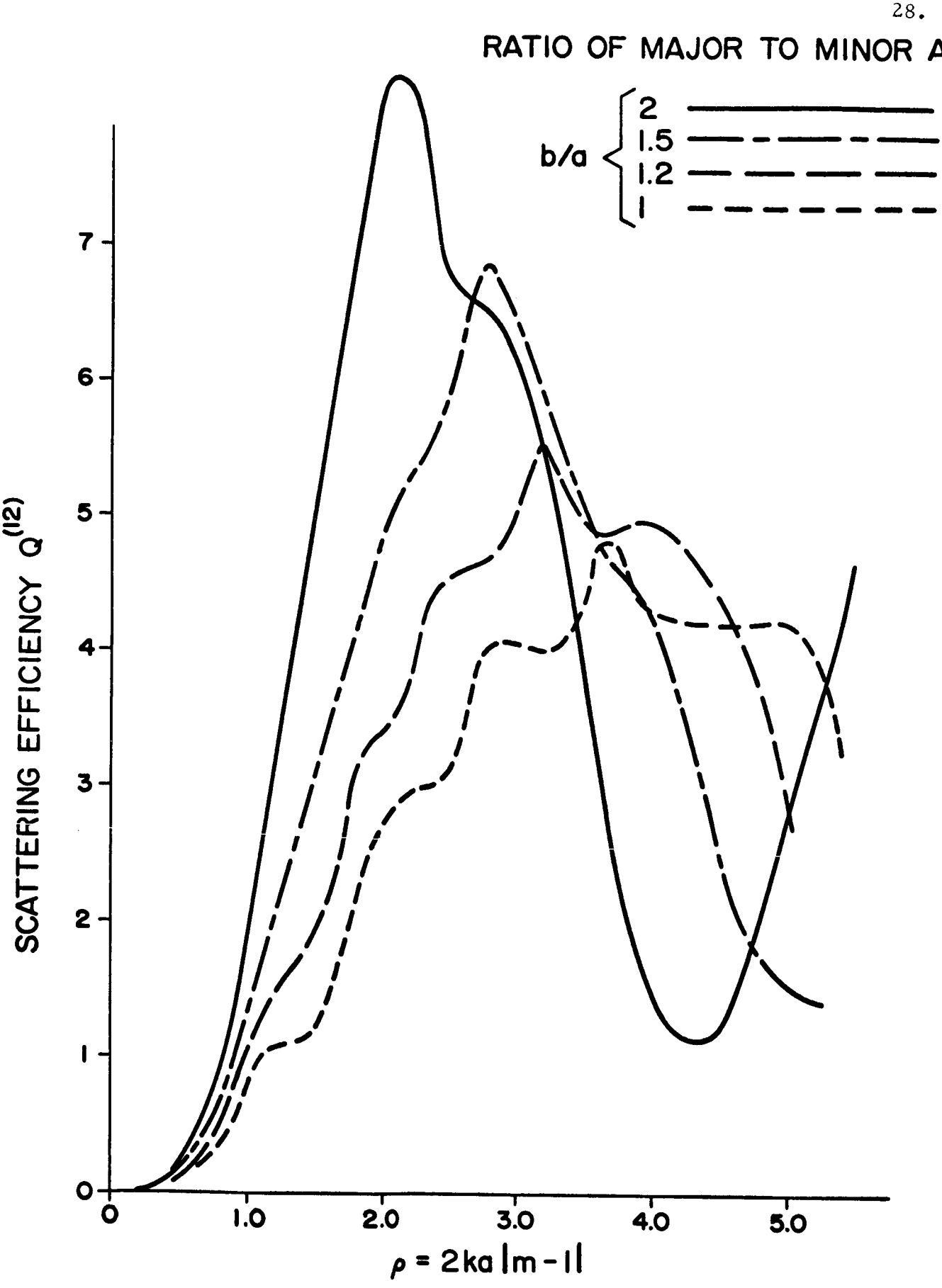

Figure 5 SCATTERING EFFICIENCIES FOR $m = 1.5$, $s = 6$

3. Scattering by Arbitrarily Oriented Infinite Dielectric Cylinders

The problem of scattering of electromagnetic radiation normally incident on a homogeneous dielectric cylinder was solved long ago by Lord Rayleigh.[8] The equivalent solution for the scattering of scalar waves was extended to the case of arbitrary incidence by Montroll and Hart[9] and later[10] extended by approximation to include inhomogeneous dielectric cylinders (actually the scalar wave analogue). Several year later Wait[11] generalized the electromagnetic scattering from a cylinder to include arbitrary orientation.

Although many calculations have been performed for the case of normal incidence, we have not been able to find any for the tilted cylinder. An extensive set of calculations are being carried out for this problem , the results of which will be published elsewhere.[12] We limit ourselves here to a demonstration of the method for obtaining the results and some examples of the calculations. We also indicate some interesting effects that occur as the cylinder is tilted.

The remainder of this section is devoted to the calculation of scattering by a dielectric cylinder in vacuum. The generalizations to include other cases will be made in a later paper.

a. Basic equations for cylinder scattering.

We follow the notation of van de Hulst.[13] Let U and V be two solutions of the scalar wave equation

$$\nabla^2\psi + m^2k^2\psi = 0 \tag{20}$$

We define the associated solutions $\underset{\sim}{M}$ and $\underset{\sim}{N}$ of the vector wave equation

by

$$\underset{\sim}{M}_{\psi} = \underset{\sim}{\nabla} \times (\hat{z}\psi)$$
$$mk\, \underset{\sim}{N}_{\psi} = \underset{\sim}{\nabla} \times \underset{\sim}{M}_{\psi} \tag{21}$$

where $\hat{z}$ is a unit vector along the cylinder axis.

The electric and magnetic fields are then given by

$$\underset{\sim}{E} = \underset{\sim}{M}_V + i\, \underset{\sim}{N}_U$$
$$\underset{\sim}{H} = m(-\underset{\sim}{M}_U + i\, \underset{\sim}{N}_V) \tag{22}$$

Referring to Figure 6 we write the solutions U and V corresponding to the "E" or "H" case; i.e., radiation linearly polarized with the electric and magnetic vector in the plane containing the cylinder axis and the propagation vector $\underset{\sim}{k}$.

	"E" case	"H" case	
$r > a$	$U = \sum_{n=-\infty}^{\infty} F_n [J_n(\ell r) - b_n^E H_n(\ell r)$	$U = \sum_{n=-\infty}^{\infty} F_n [-b_n^H H_n(\ell r)$	(23)
	$V = \sum_{n=-\infty}^{\infty} F_n [-a_n^E H_n(\ell r)$	$V = \sum_{n=-\infty}^{\infty} F_n [J_n(\ell r) - a_n^H H_n(\ell r)$	
$r < a$	$U = \sum_{n=-\infty}^{\infty} F_n d_n^E J_n(\ell_1 r)$	$U = \Sigma F_n d_n^H J_n(\ell_1 r)$	(24)
	$V = \sum_{n=-\infty}^{\infty} F_n c_n^E J_n(\ell_1 r)$	$V = \Sigma F_n c_n^H J_n(\ell_1 r)$	

where

$$F_n = (-i)^n \exp(i\omega t - i k z \sin\alpha + i n \theta)$$
$$\ell = k \cos\alpha, \quad \ell_1 = k\sqrt{m^2 - \sin^2\alpha}, \quad \alpha = \frac{\pi}{2} - \chi$$

a = radius of cylinder

J_n = cylindrical Bessel function of the first kind

H_n = cylindrical Hankel function of the second kind.

Applying the appropriate boundary conditions on E and H at the surface of the cylinder we obtain the coefficients a_n, b_n, c_n, d_n,

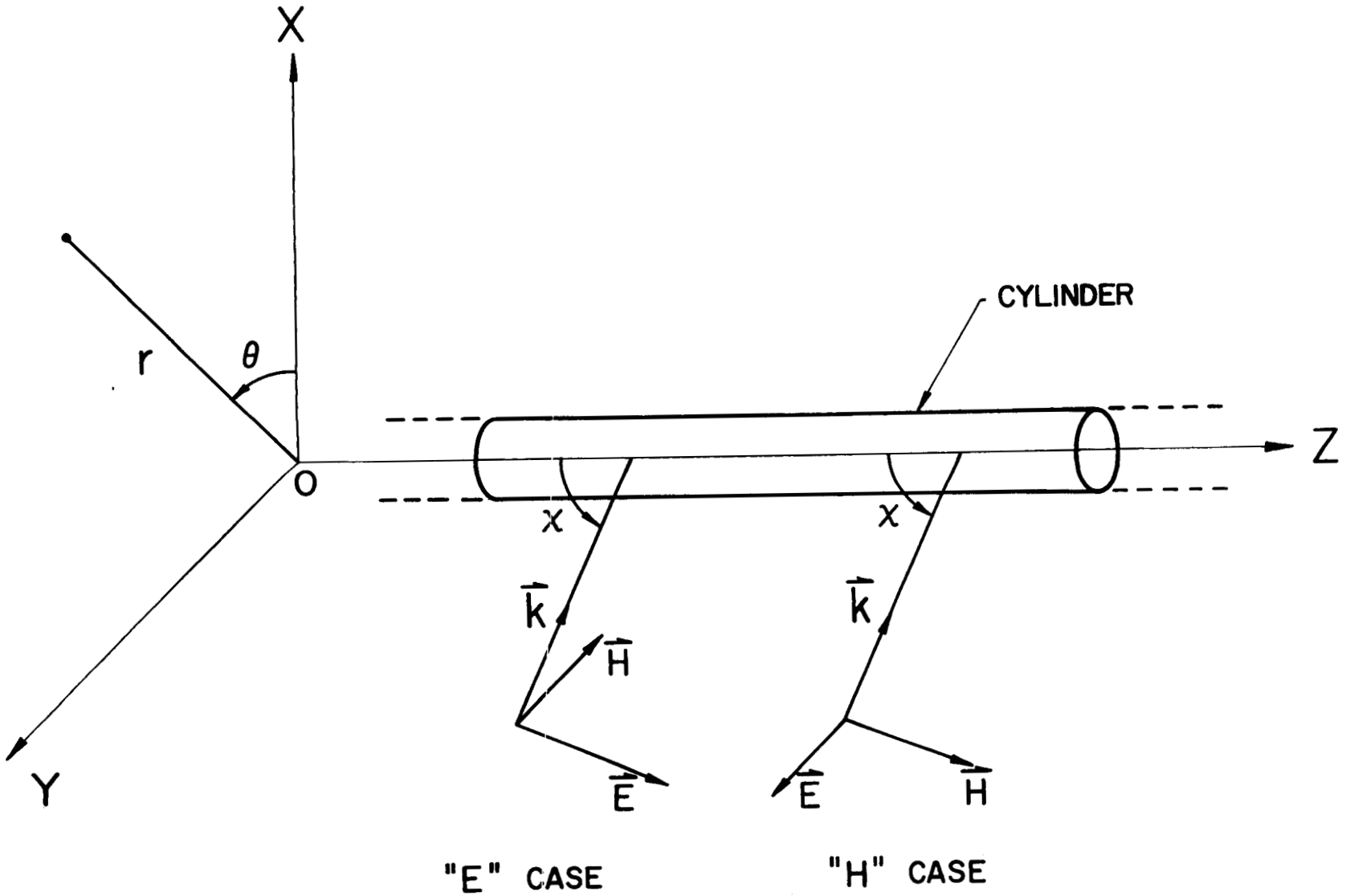

FIG. 6 Coordinates and orientation of vectors used in describing the scattering by infinite cylinder. The "E" (or "H") case is that in which $\vec{E}$(or $\vec{H}$), $\vec{k}$ and the cylinder axis are coplanar.

"E"

$$a_n^E = i\, n \sin\alpha\, S\, R_n \frac{B_n(\mu) - A_n(\mu)}{A_n(\epsilon)\, A_n(\mu) - n^2 S^2 \sin^2\alpha}$$

$$b_n^E = R_n \frac{A_n(\mu)\, B_n(\epsilon) - n^2 S^2 \sin^2\alpha}{A_n(\epsilon)\, A_n(\mu) - n^2 S^2 \sin^2\alpha}$$

$$c_n^E = -\sqrt{\mu}\, \frac{(\ell a)^2 H_n(\ell a)}{(\ell_1 a)^2 J_n(\ell_1 a)}\, a_n^E$$

$$d_n^E = \sqrt{\epsilon}\, \frac{(\ell a)^2}{(\ell_1 a)^2 J_n(\ell_1 a)} \left[J_n(\ell a) - H_n(\ell a)\, b_n^E\right]$$

"H"

$$a_n^H = R_n \frac{A_n(\epsilon)\, B_n(\mu) - n^2 S^2 \sin^2\alpha}{A_n(\epsilon)\, A_n(\mu) - n^2 S^2 \sin^2\alpha}$$

$$b_n^H = -\, a_n^E$$

$$c_n^H = \sqrt{\mu}\, \frac{(\ell a)^2}{(\ell_1 a)^2 J_n(\ell_1 a)} \left[J_n(\ell a) - H_n(\ell a)\, a_n^H\right]$$

$$d_n^H = -\sqrt{\epsilon}\, \frac{(\ell a)^2 H_n(\ell a)}{(\ell_1 a)^2 J_n(\ell_1 a)}\, b_n^H \qquad (25)$$

where

$$S = (\ell a)^{-2} - (\ell_1 a)^{-2}\ ; \quad R_n = J_n(\ell a) \big/ H_n(\ell a)$$

$$A_n(\xi) = \frac{H_n'(\ell a)}{\ell a\, H_n(\ell a)} - \xi\, \frac{J_n'(\ell_1 a)}{\ell_1 a J_n(\ell_1 a)}\ ; \quad B_n(\xi) = \frac{J_n'(\ell a)}{\ell a\, J_n(\ell a)} - \xi\, \frac{J_n'(\ell_1 a)}{\ell_1 a J_n(\ell_1 a)}$$

The extinction efficiencies (using the optical theorem) and the scattering efficiencies obtained by integrating the differential scattering cross-section are given by

$$Q^{E}_{ext} = \frac{C^{E}_{ext}}{2a} = \frac{2}{ka} \text{ Re } \left\{ b^{E}_{0} + 2\sum_{n=1}^{\infty} b^{E}_{n} \right\} \quad (26)$$

$$Q^{H}_{ext} = \frac{C^{H}_{ext}}{2a} = \frac{2}{ka} \text{ Re } \left\{ a^{H}_{0} + 2\sum_{n=1}^{\infty} a^{H}_{n} \right\} \quad (27)$$

$$Q^{E}_{sca} = \frac{C^{E}_{sca}}{2a} = \frac{2}{ka} \left[|b^{E}_{0}|^{2} + 2\sum_{n=1}^{\infty} (|b^{E}_{n}|^{2} + |a^{E}_{n}|^{2}) \right] \quad (28)$$

$$Q^{H}_{sca} = \frac{C^{H}_{sca}}{2a} = \frac{2}{ka} \left[|a^{H}_{0}|^{2} + 2\sum_{n=1}^{\infty} (|a^{H}_{n}|^{2} + |b^{H}_{n}|^{2}) \right] \quad (29)$$

When the index of refraction is real $Q_{ext} = Q_{sca}$. All of the above (Eqs. 26 - 29) apply to unit length of cylinder.

The case of arbitrary orientation of the cylinder axis relative to the $\underset{\sim}{k}$, $\underset{\sim}{E}$, and $\underset{\sim}{H}$ of an incident electromagnetic wave of arbitrary state of polarization can be made up of a linear superposition of the basic "E" case and "H" case solutions with appropriate amplitudes and phases (see Eq. (34)).

b. Numerical results for the tilted cylinder

The calculations have been made for cylinders with real index of refraction m = 1.6 which corresponds to the index of refraction of lucite for microwaves. As a numerical check, Q_{ext} and Q_{sca} were independently evaluated.

In Fig. 7 we have plotted the complex expressions

$$\frac{2}{ka} \left\{ b^{E}_{0} + 2\sum_{n=1}^{\infty} b^{E}_{n} \right\} \quad \text{and} \quad \frac{2}{ka} \left\{ a^{H}_{0} + 2\sum_{n=1}^{\infty} a^{H}_{n} \right\}$$

the projections on the real axis being the extinction efficiencies. The cylinder for which ka = 0.7 is rather thin and it is to be expected that for normal incidence only a few terms in the expansions are required. This is indeed the case. Furthermore as the propagation

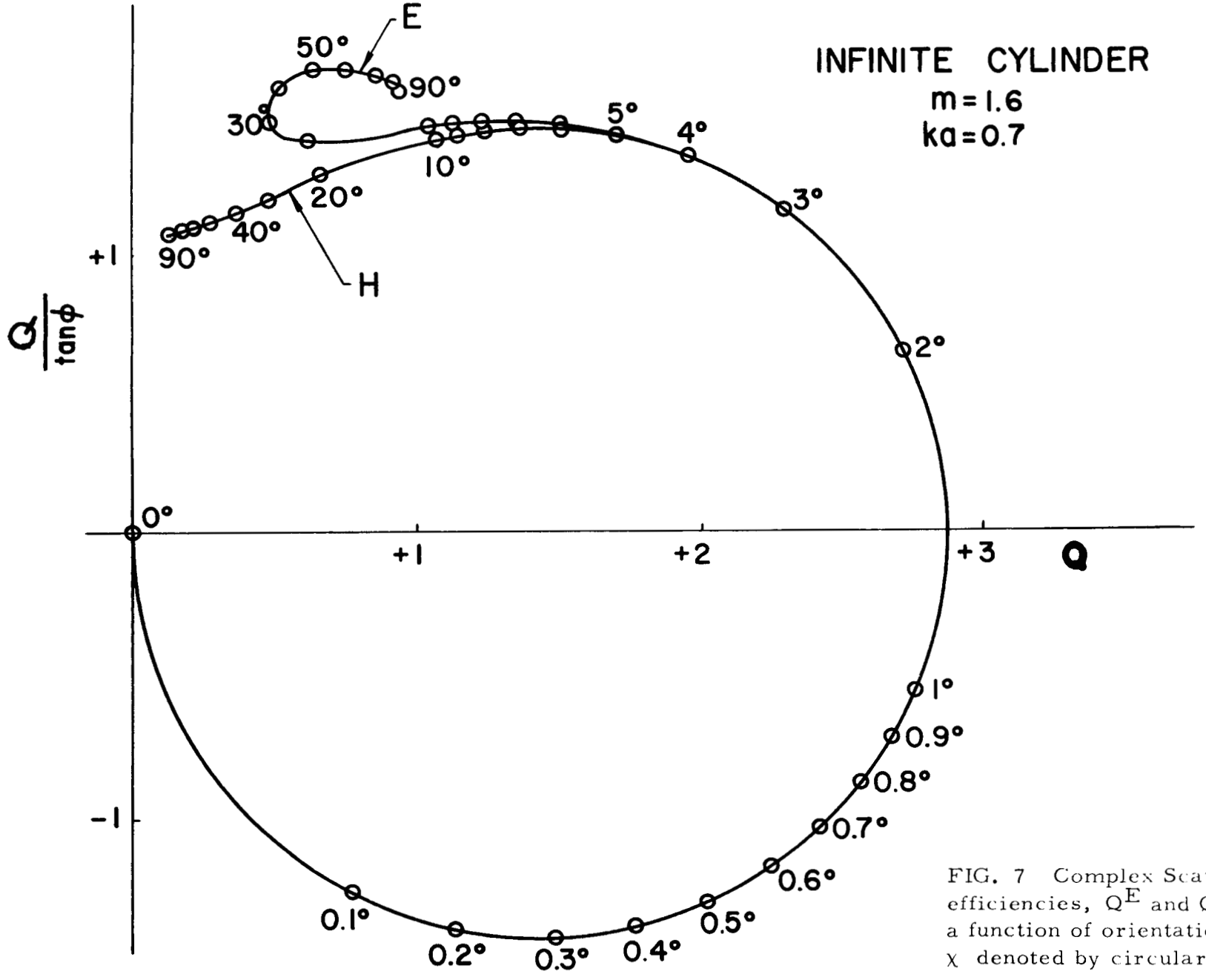

FIG. 7 Complex Scattering efficiencies, Q^E and Q^H as a function of orientation angle χ denoted by circular points.

direction approaches the direction of the cylinder axis ($\chi \to 0^{\circ}$, $\alpha \to 90^{\circ}$), only the n = 1 terms for the "E" case and the "H" case are important. It can be shown that as $\chi \to 0^{\circ}$

$$\frac{4}{ka} b_1 = \frac{4}{ka} a_1 \underset{\chi \to \infty}{\to} \frac{2}{ka} \left\{ 1 - \frac{i}{2\pi} \left[4 \ln \ell a - .6159 + 4 (\ell_1 a)^2 + 2 (\epsilon + \mu) \frac{J_1'(\ell_1 a)}{(\ell_1 a) J_1(\ell_1 a)} \right]^{-1} \right\} \qquad (30)$$

This is the equation for a circle whose center is at $(ha)^{-1}$ and whose radius is $(ka)^{-1}$. We see, then, that as both $\chi \to 0^{\circ}$ and $ka \to 0$ the extinction efficiency will, for some small χ, become very large. It should be pointed out, however, that the cross-section must eventually go to zero at grazing incidence.

We show, in Fig. 8, the extinction efficiency as a function of orientation for the same cylinder (ka = 0.7) represented by Fig. 7.

The computations for a slightly larger cylinder (ka = 0.8) are shown in Fig. 9. The very interesting feature to be noted here is the crossover of the Q^E and Q^H curves. The crossover of Q^E and Q^H (polarization reversal) for large cylinders and normally incident radiation has been known (Dubois effect[14]) for a long time. However, the effect shown in Fig. 8 is quite different in that it shows up for small cylinders and is a function of their orientation.

As one increases the cylinder diameter, more and more terms are required in the expansion and, as a consequence, the n = 1 term is no longer dominant except for extremely small values of χ. This is shown in Fig. 10 where the circular form of the complex

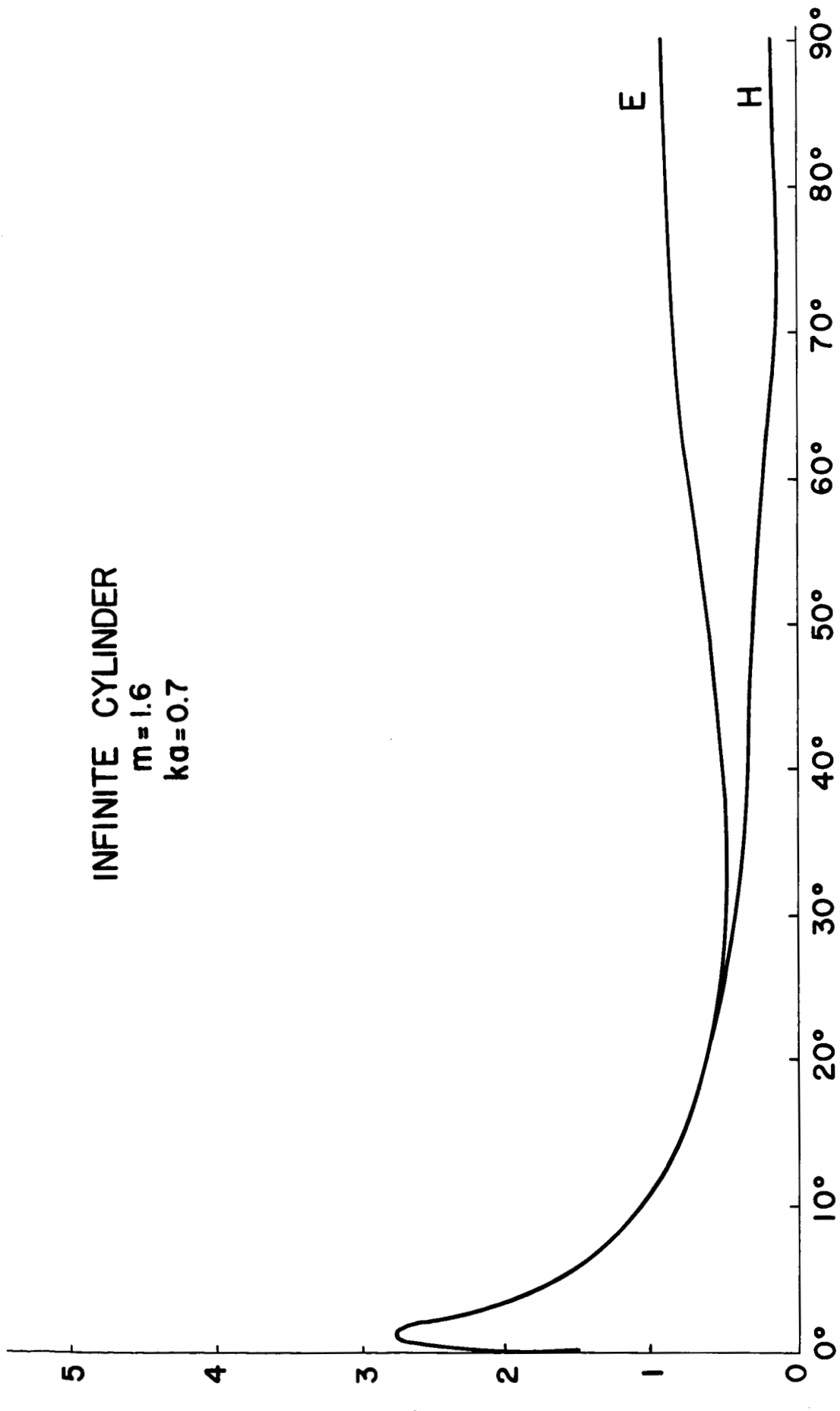

FIG. 8 Scattering efficiencies Q^E and Q^H as a function of orientation angle.

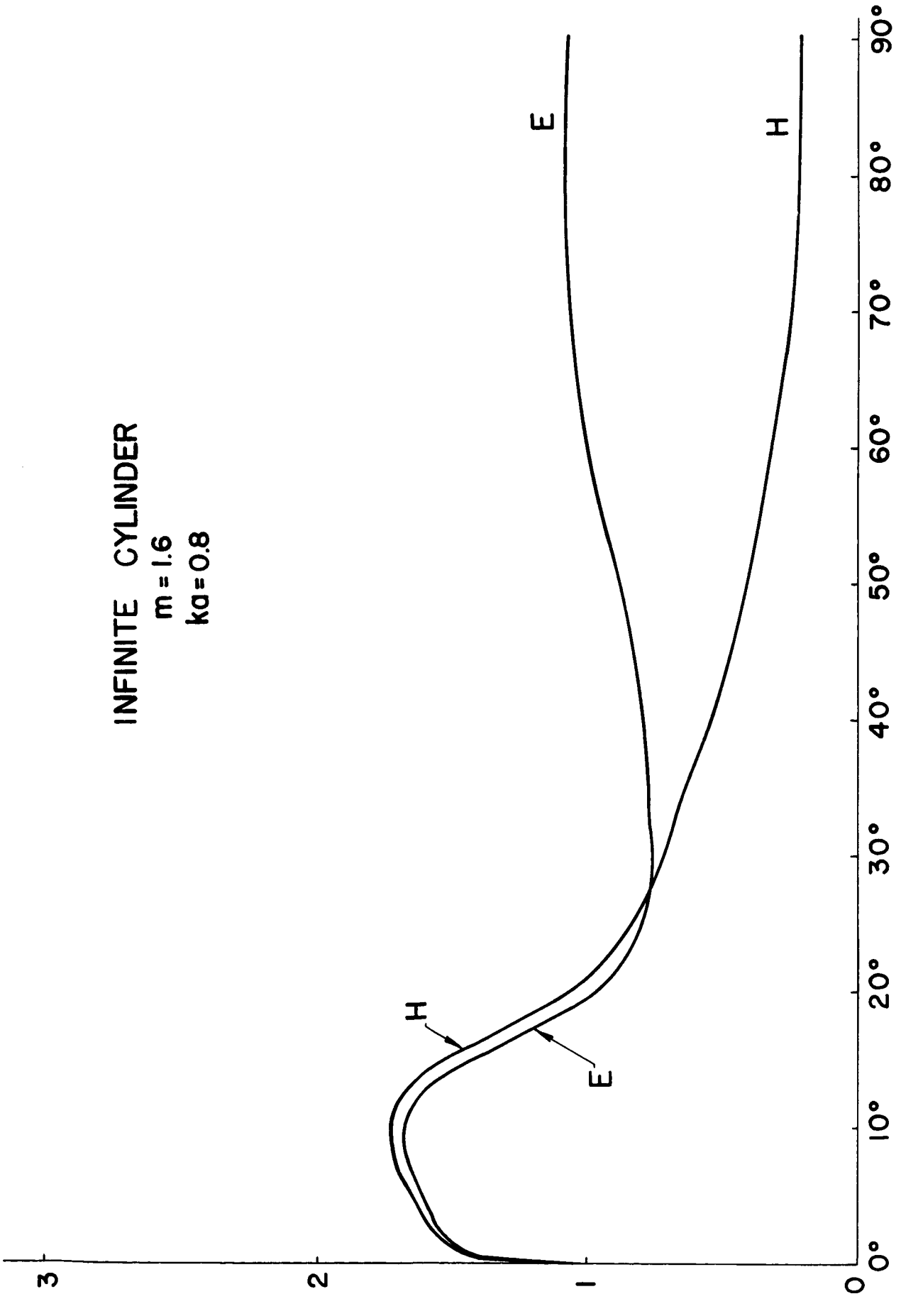

FIG. 9 Scattering efficiencies Q^E and Q^H as a function of orientation angle.

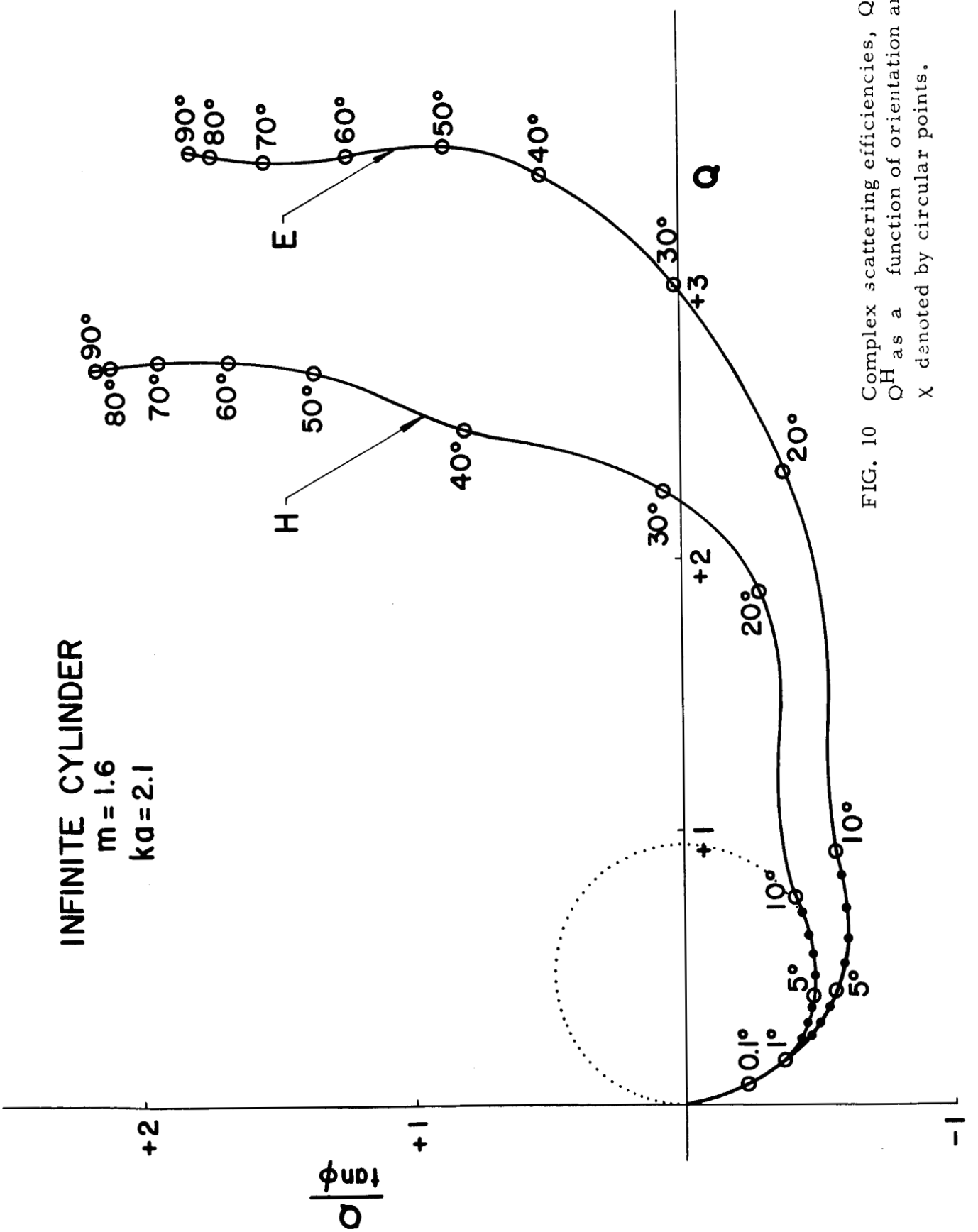

FIG. 10 Complex scattering efficiencies, Q^E and Q^H as a function of orientation angle χ denoted by circular points.

extinction has almost vanished. It can be seen in Fig. 11 that for $ka > 1$ the values of Q^E and Q^H become relatively insensitive to cylinder tilt angle and that also $Q^E - Q^H$ is fairly constant.

Finally in Fig. 12 we see some samples of the variations of the extinction Q^E with size for tilt angles $\chi = 1^o$ and $\chi = 10^0$. For normal incidence ($\chi = 90^o$) one obtains a curve which (except for a few wiggles) rises uniformly to a maximum at $2ka(m - 1) \approx 4$ ($ka = 3.3$ in our case) then decreases for a rather considerable distance in ka.

A comment on angular scattering distribution is perhaps in order. It should be noted that the scattered radiation is confined to a cone whose half angle is the angle χ. In other words, for the infinite cylinder there is no true back scattering even though there is radiation appearing at $\theta = 180^o$.

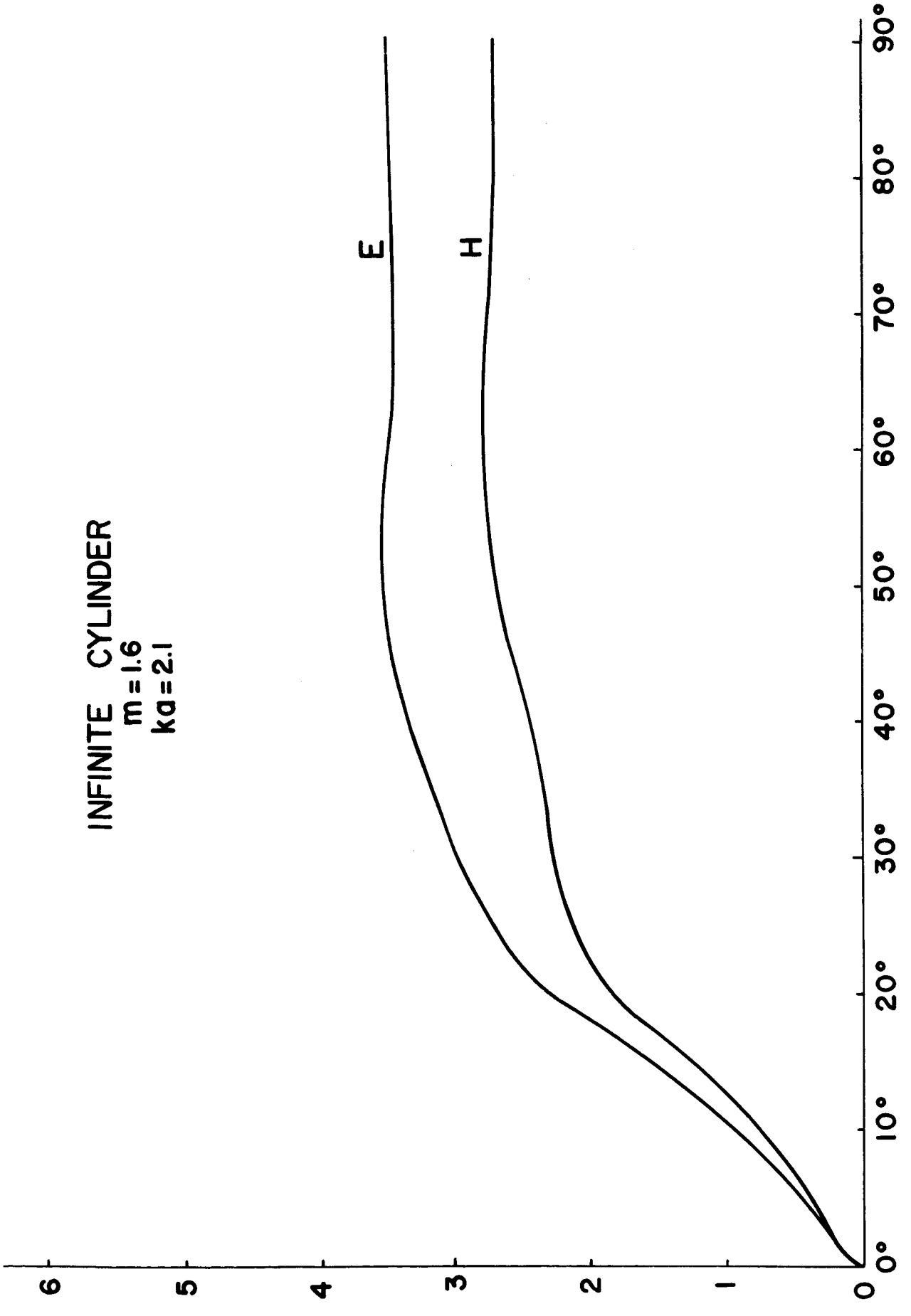

FIG. 11 Scattering efficiencies, Q^E and Q^H, as a function of orientation angle.

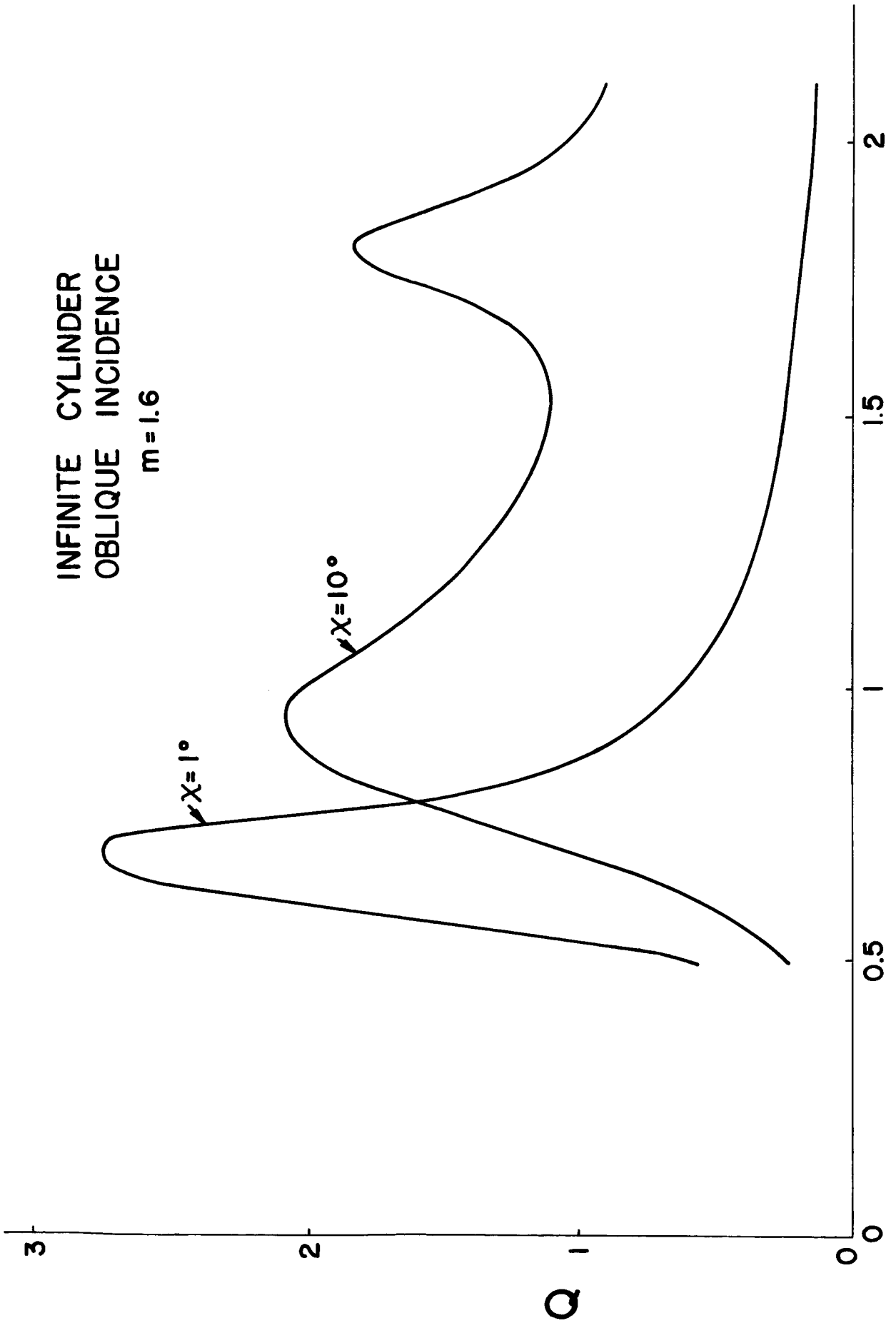

FIG. 12 Scattering efficiency Q^E as a function of ka showing increasing resonance for increasing tilt.

4. Microwave Scattering

A preliminary account of this work which consists of a new and improved method for obtaining detailed information on the extinction cross sections for scattering of 3 cm microwaves by arbitrarily oriented particles has appeared elsewhere.[15] More detailed exposition of the experimental method is being prepared for publication. We present here an enlarged abstract along with some of the results in order to demonstrate the usefulness of the experimental approach to the scattering problem. It should be remembered that in practice the problems we are faced with can not entirely be solved by consideration of simple particle shapes and that, as of this moment, only the scattering of a scalar wave propogated along the axis of an axially symmetric particle has yielded numerical results. The theoretical calculation of the general case of scattering of electromagnetic radiation for arbitrary particle orientation, at least by a method similar to that in section 2 of this paper, while feasible would be enormously expensive for sizes (relative to wave length) which can readily yield good experimental results.

a. Theoretical Basis for the Measurements

The experimental determination of the total (extinction) cross section including both scattering and absorption is conveniently done by measuring the forward scattering amplitude employing the optical theorem, the vector form of which is[16]

$$C_{ext} = (4\pi/k^2)\ \underset{\sim}{q} \cdot \underset{\sim}{f}_{\underset{\sim}{q}} \sin\ \varphi \qquad (31)$$

where $\underset{\sim}{f}\,\underset{\sim}{q}\,e^{i\varphi}$ is the complex vector amplitude in the forward direction for incident radiation polarized along the direction of the unit vector $\underset{\sim}{q}$.

Although Figure 6 could in principle be referred to at this point, it seems desirable for clarity to present a somewhat different realization in Figure 13. Again the angle χ is used to describe the orientation of the symmetry axes relative to the direction of propagation. The angle between the direction of polarization and the plane containing $\underset{\sim}{k}$ and the symmetry axis is called ψ.

We denote the forward scattering amplitude when $\psi = 0^{\circ}$ as $f_E(\chi)$ and when $\psi = 90^{\circ}$ as $f_H(\chi)$. Due to the symmetry of our scatterers it is necessary to know only the cross section in these two mutually perpendicular planes; i.e., the $\underset{\sim}{E}$ - $\underset{\sim}{k}$ plane and the $\underset{\sim}{H}$ - $\underset{\sim}{k}$ plane in order to fully describe the case for arbitrary orientation.

The scattering amplitude for a particle oriented as in Figure 13 is given by

$$f(\chi, \psi) = [\, f_E(\chi) \cos^2\psi + f_H(\chi) \sin\psi \,]\, \underset{\sim}{i} + [\, f_E(\chi) - f_H(\chi) \,] \sin\psi \cos\psi \, \underset{\sim}{j} \tag{32}$$

where $\underset{\sim}{i}$ and $\underset{\sim}{j}$ are unit vectors along the x and y direction respectively. The optical theorem then gives

$$C_{ext}(\chi, \psi) = \frac{4\pi}{k^2} [\, f_E(\chi) \sin\varphi_E(\chi) \cos^2\psi + f_H(\chi) \sin\varphi_H(\chi) \sin^2\psi \,] \tag{33}$$

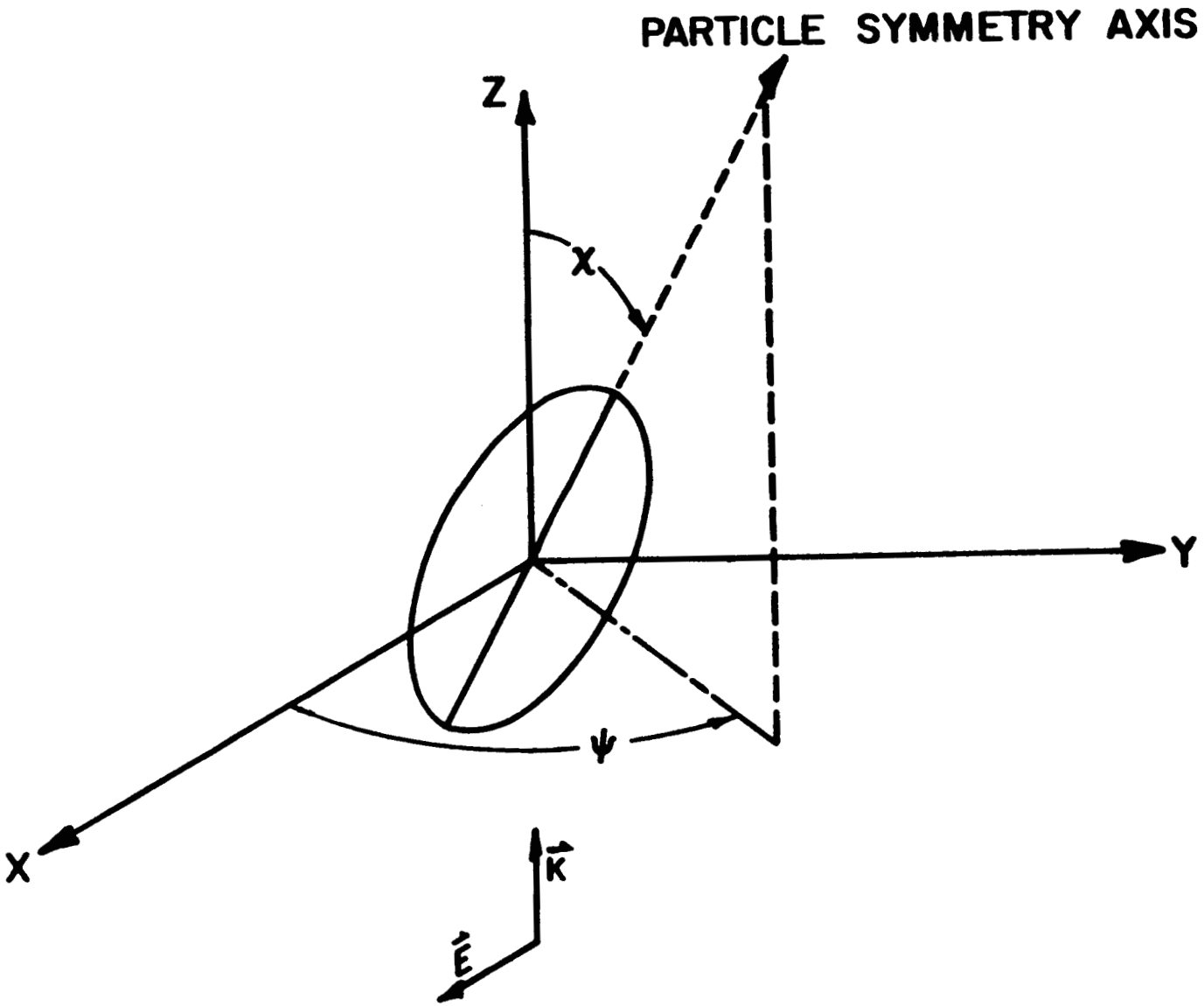

FIG. 13

or, in the notation of section 3 for extinction efficiencies,

$$Q_{ext}(\chi, \psi) = Q^{E}(\chi) \cos^2\psi + Q^{H}(\chi) \sin^2\psi \qquad (34)$$

b. Experimental Procedure

Essentially the experimental procedure consists in first nulling out the received incident radiation when no target is present and then displaying graphically on an X - Y plotter the real and imaginary components of the additional signal produced by a target.

In Figure 14 is shown a reproduction of an X - Y chart recording for a typical run. The curves labelled kE and kH represent the locus of the complex forward scattering amplitudes as the particle orientation is charged (vary χ) within the two mutually perpendicular planes previously mentioned. The dots along the curves are put in by hand as the target orientation mechanism is stopped at the designated angles. The origin from which the complex scattering amplitudes are measured is determined by rapidly lowering the target and noting the final position on the X - Y plotter. The line labelled "Target Dropping" is a tracing of the X - Y pen as the scatterer is lowered out of the incident beam. In order to normalize and orient the scattering amplitudes one experimentally locates the point which defines the complex scattering amplitude for a sphere of known size and index of refraction. A Mie theory calculation for the scattering by the sphere gives the phase (φ_{calc} in the Figure) and the amplitude ($|f_{calc}|$).

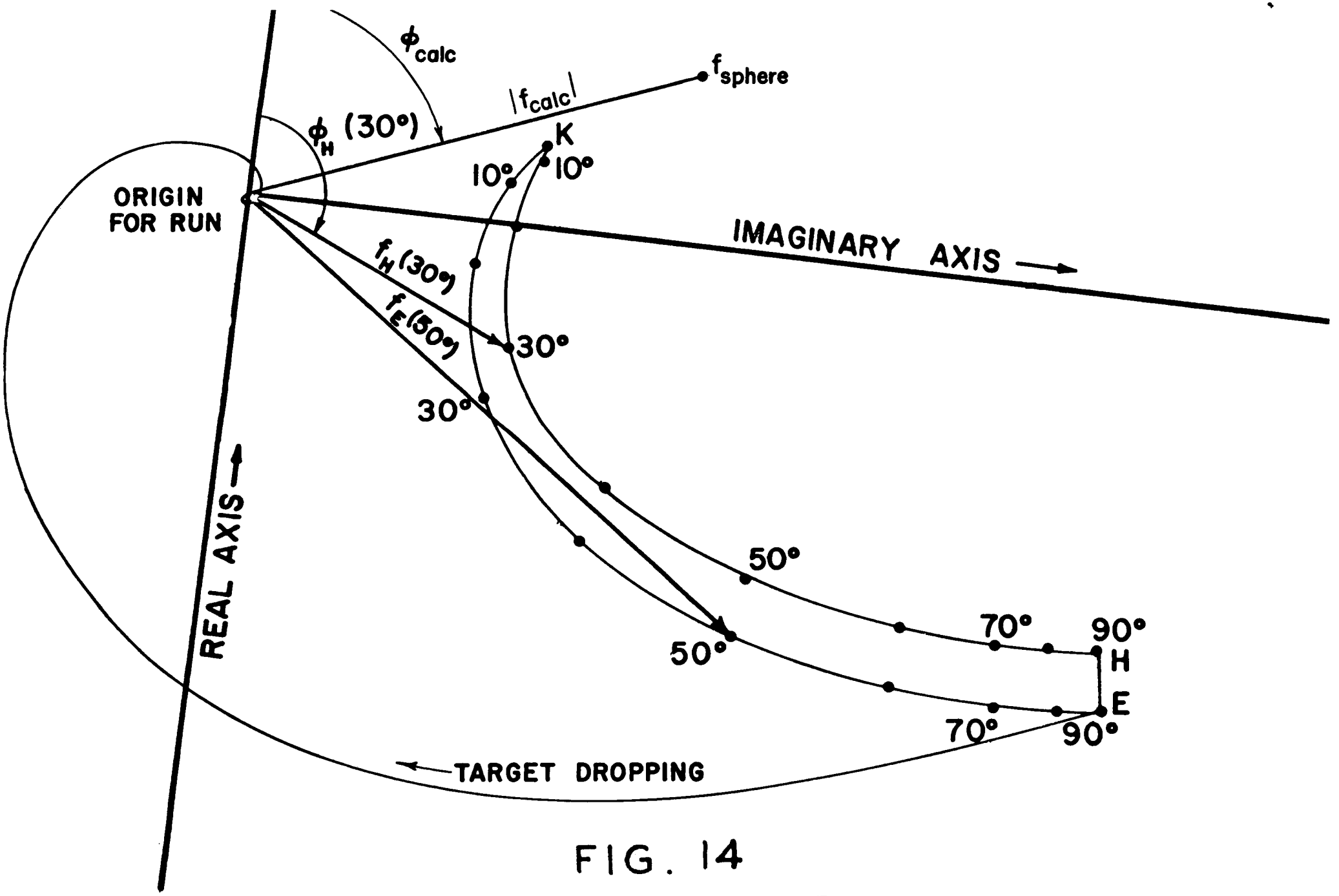

FIG. 14

TYPICAL DATA RUN

SHOWING VECTOR SCATTERING AMPLITUDES AT VARIOUS ORIENTATIONS

The phase, φ_{calc}, is used to orient the real and imaginary axes, and the amplitude $|f_{calc}|$, defines the absolute scale in the X - Y plane. In order to eliminate the possibilities of systematic errors which could be introduced if a particular sphere is inaccurately manufactured, we perform the actual normalization by averaging over a set of "standard" spheres.

The repeatability and the internal consistency of the measurements have been quite good with deviations of less than 2 percent in the magnitude and 3^{o} in phase of the forward scattering amplitude.

It can be seen that the experimental data appears naturally in exactly the same form as that which we have used in Figures 7 and 10 for the theoretical results on the cross section of infinite cylinders. This manner of presentation of the raw data makes it possible to detect and measure subtle differences in scattering produced by orientation changes and is perhaps the most important feature of our new experimental procedure.

c. Results

Figure 15 is shown as an example of the information which can be extracted from the raw data. We have plotted here the real and imaginary components as well as the absolute value and phase of the forward scattering amplitude for a prolate spheroid as a function of its orientation. The degree of internal consistency of the experimental method may be inferred from the smoothness of the curves.

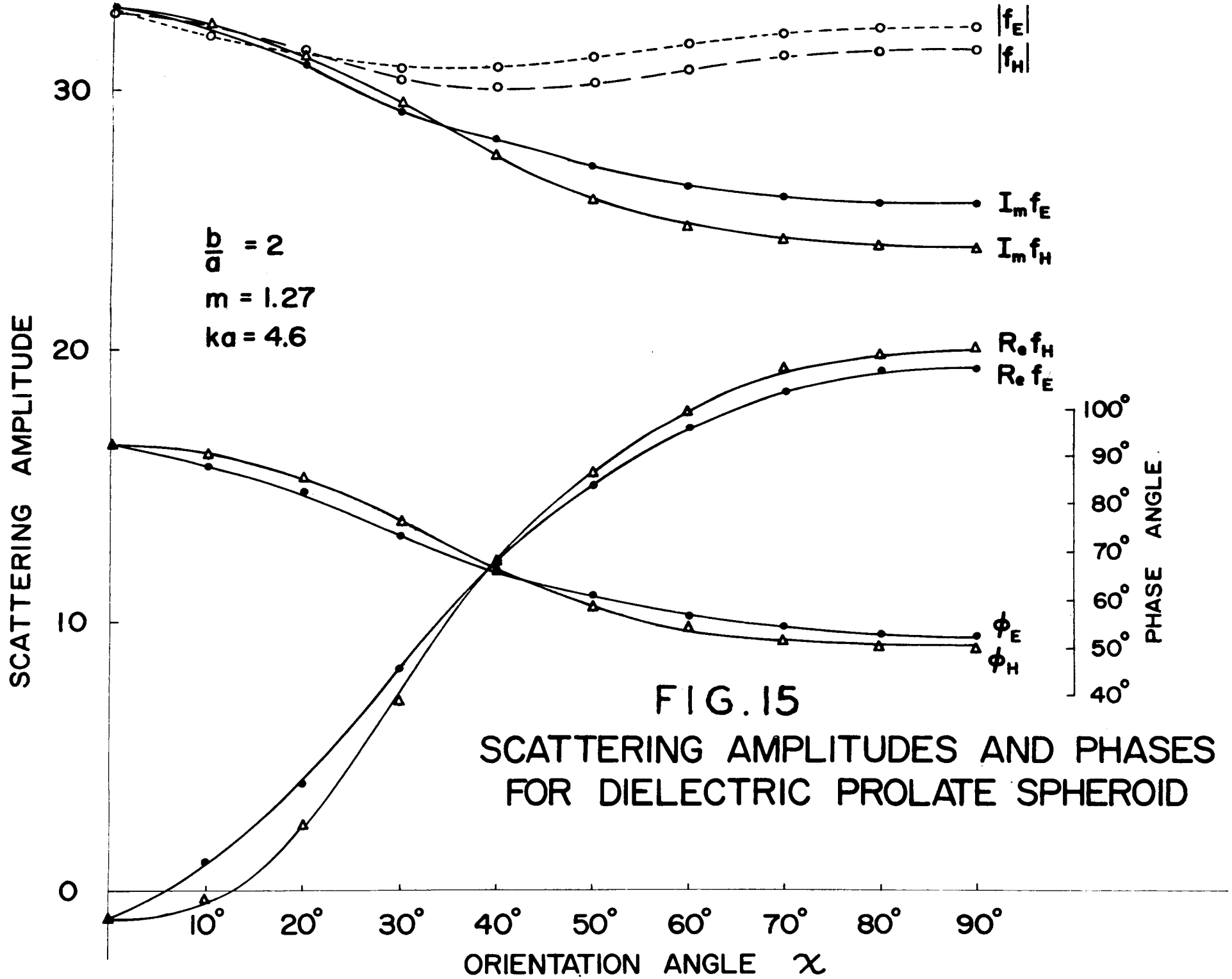

FIG. 15

SCATTERING AMPLITUDES AND PHASES FOR DIELECTRIC PROLATE SPHEROID

As is well known the Rayleigh approximation becomes rapidly poorer as ka exceeds unity. This is clearly demonstrated in Figure 16 where total cross sections are shown for a prolate spheroid which while still fairly small has ka = 2.5. The Rayleigh approximation is incorrect by a factor of 5. On the other hand a low index of refraction scalar approximation[6] is in remarkably good agreement (less than 3 percent difference from Q^E) in spite of the fact that m = 1.255 is certainly not very close to one. It had been shown by van de Hulst[17] that this kind of agreement is not unusual for spheres but as has already been stated in section 2 the agreement for spheroids may become particularly poor for certain values of ka; namely, the values of ka which define the major extinction resonance for axially incident radiation. It turns out that ka = 2.5 is sufficiently below this value of ka $\approx$ 4. One should expect the agreement between the low index scalar wave approximation to be poor for ka = 4.6 (defining the spheroid of Figure 15) and this is indeed the case. It is rather interesting and important in some applications to note that the polarization ratio Q^E/Q^H obtained experimentally for the ka = 2.5 spheroid is very close to that obtained from the Rayleigh approximation, and is not too different from that for the infinite cylinder with ka = 2.1 (See Figure 11).

For the largest spheroid with ka = 10.1 it is reasonable to compare the results with those predicted by the geometrical optics limit as well as those given by the ray approximation. Therefore, in Figure 17 along with

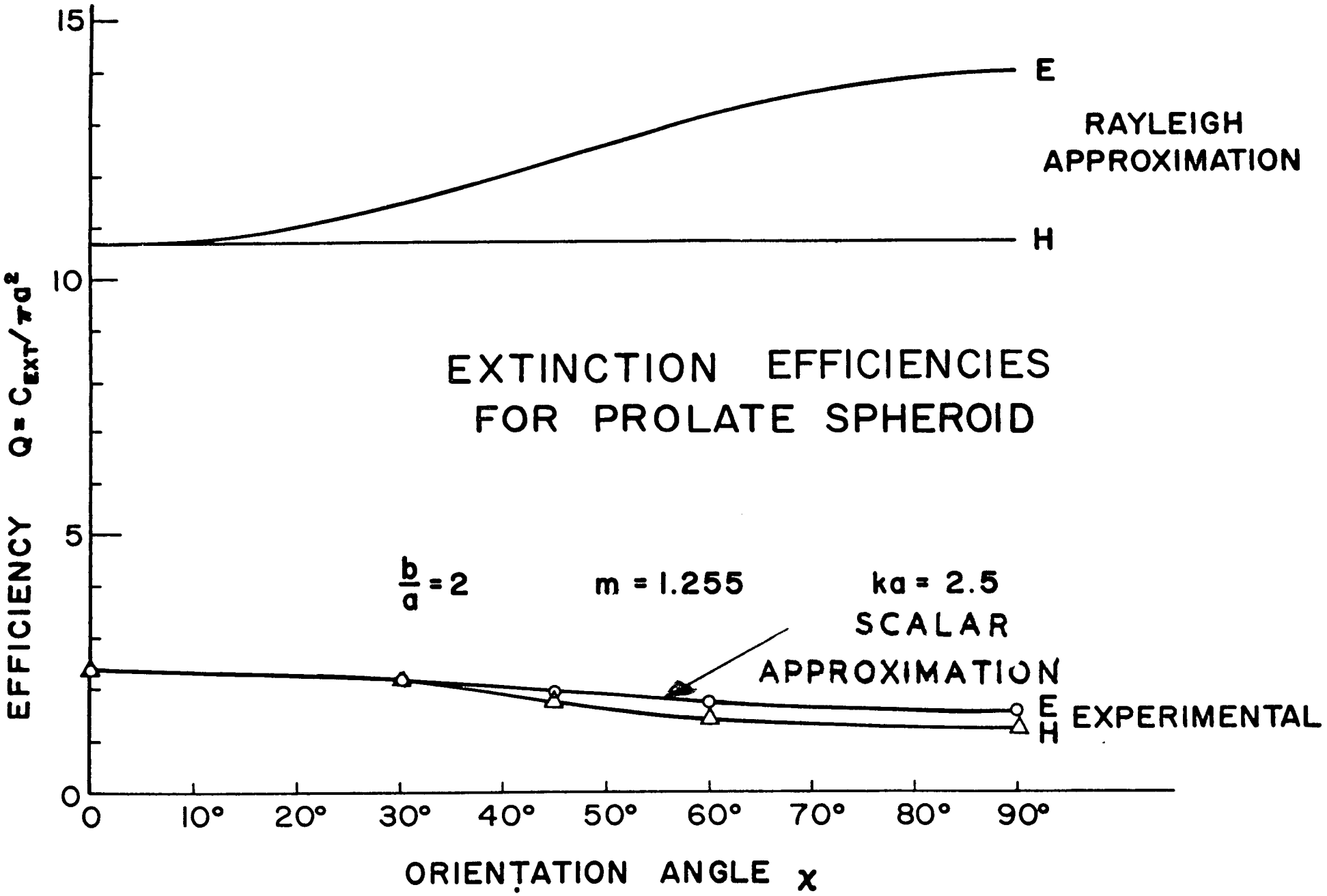
15
10
5
0
E
H
RAYLEIGH
APPROXIMATION
EXTINCTION EFFICIENCIES
FOR PROLATE SPHEROID
EFFICIENCY Q = C_EXT/πa²
b/a = 2
m = 1.255
ka = 2.5
SCALAR
APPROXIMATION
E/H EXPERIMENTAL
0
10°
20°
30°
40°
50°
60°
70°
80°
90°
ORIENTATION ANGLE χ

FIG. 16

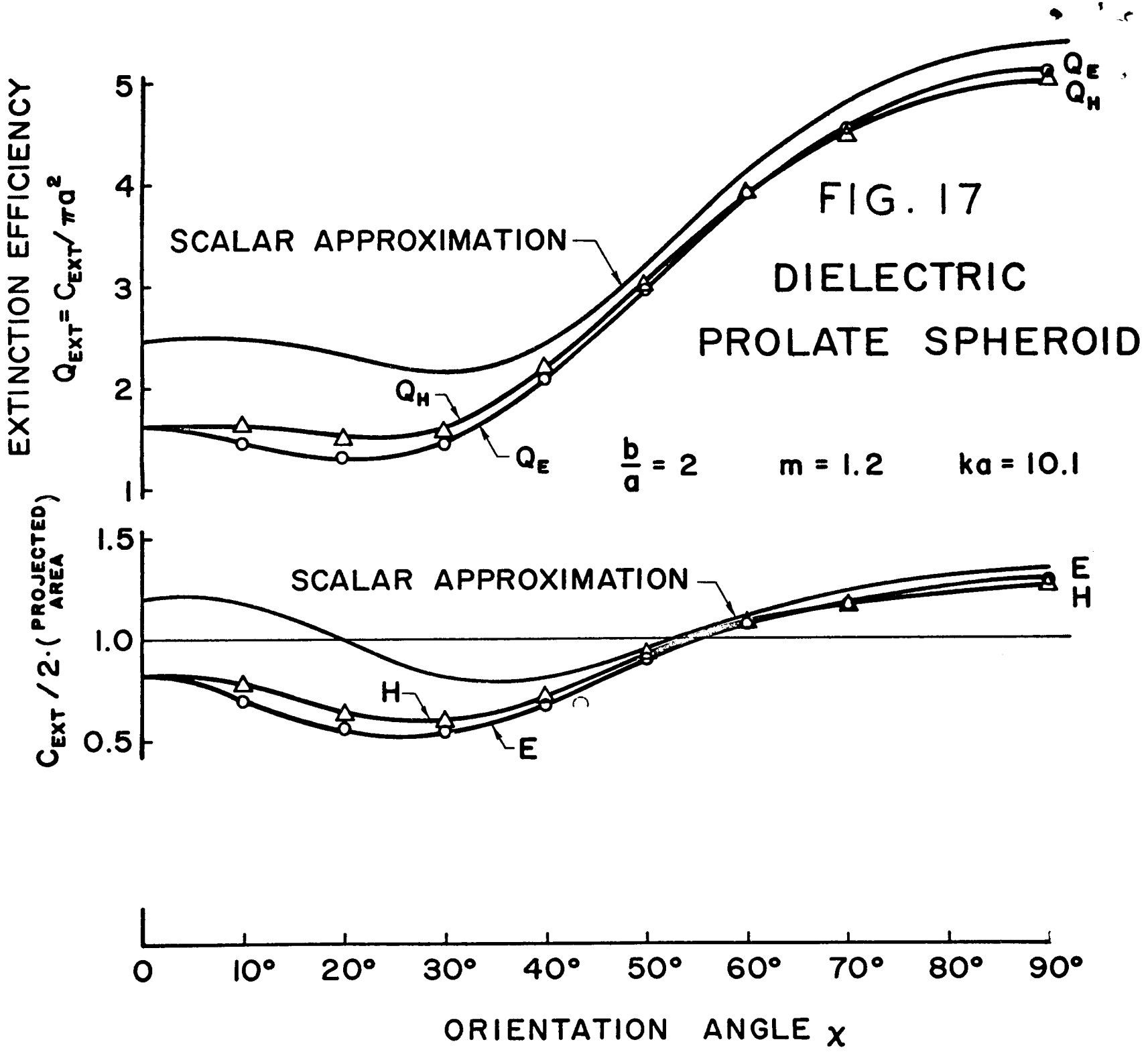

FIG. 17

DIELECTRIC

PROLATE SPHEROID

a curve for the extinction efficiency, a curve is plotted for the extinction cross section divided by the geometric optics cross section; i. e., twice the projected area presented by the spheroid to the incident radiation. This quantity oscillates around the value 1 for different orientations. The ray approximation is in partial agreement with the experimental results for ka = 10.1 in that it gives a very similar dependence of cross section on orientation. The agreement is certainly not as good as that for ka = 2.5 although it is probably satisfactory for semi-quantitative calculations.

Acknowledgements

One of us (J. M. G.) would like to express his sincere appreciation to Professor J. Robert Oppenheimer for the hospitality extended to him at The Institute for Advanced Study.

References

1. van de Hulst, H. C. (1957) "Light Scattering by Small Particles", J. Wiley and Sons, Inc., New York, p.132.
2. Lord Rayleigh (1897) Phil. Mag. Series 5, 44, p. 28.
3. Lord Rayleigh (1910) Proc. Roy Soc. London Ser. A, 84, p. 25
   (1914) Proc. Roy. Soc. London Ser. A, 90, p. 219.
   Gans, R., (1925) Ann. Phys. 76, p. 29.
   Born, M. (1926) Ziet. Phys. 37, p. 863; 38, p. 803.
4. Libelo, L. F., 1964, Ph. D. Thesis, Rensselaer Polytechnic Institute.
5. Mie, G. (1908) Ann. Phys. 25, p. 37.
6. Greenberg, J. M. (1960), Appl. Phys. 31, p. 82.
7. Greenberg, J. M., Pedersen, N. E. and Pedersen, J. C. (1961) J. Appl. Phys. 32, p. 233.
8. Lord Rayleigh (1918), Phil. Mag 36, p. 365.
9. Montroll, E. W. and Hart, R. W. (1951) J. Appl. Phys., 22, p.1278.
10. Montroll, E. W. and Greenberg, J. M. (1952), Phys. Rev. 86, p. 889.
11. Wait, J. R. (1955) Can. J. Phys., 33, p. 189.
12. Lind, A. C. and Greenberg, J. M., to be published.
13. Ref. 1. p. 297.
14. Ibid p. 322.
15. Lind, A. C., Wang, R. T., and Greenberg, J. M. (1965), J. Appl. Optics.
16. Saxon, D. S., (1955), Phys. Rev. 32, p. 233.
17. van de Hulst, H. C. (1946) Recherches astron Obs. d' Utrecht, 11, part 1, (1948) 11 part 2.